

# ESTIMATING EXTREMAL DEPENDENCE IN UNIVARIATE AND MULTIVARIATE TIME SERIES VIA THE EXTREMOGRAM

Richard A. Davis<sup>1</sup>, Columbia University  
Thomas Mikosch, University of Copenhagen  
Ivor Cribben, Columbia University

**Abstract.** Davis and Mikosch [7] introduced the extremogram as a flexible quantitative tool for measuring various types of extremal dependence in a stationary time series. There we showed some standard statistical properties of the sample extremogram. A major difficulty was the construction of credible confidence bands for the extremogram. In this paper, we employ the stationary bootstrap to overcome this problem. Moreover, we introduce the cross extremogram as a measure of extremal serial dependence between two or more time series. We also study the extremogram for return times between extremal events. The use of the stationary bootstrap for the extremogram and the resulting interpretations are illustrated in several univariate and multivariate financial time series examples.

arXiv:1107.5592v1 [stat.ME] 27 Jul 2011

---

<sup>1</sup>coordinating author: Department of Statistics, 1255 Amsterdam Avenue, Columbia University, New York, NY 10027, USA; email: rdavis@stat.columbia.edu

*Keywords:* Extremogram, extremal dependence, stationary bootstrap, financial time series.

*Primary JEL Classification Code:* C50.

## 1. INTRODUCTION

With the wild swings recently seen in the financial markets and climatic conditions, there has been renewed interest in understanding and modeling extreme events. The extremogram, developed in Davis and Mikosch [7], is a flexible tool that provides a quantitative measure of dependence of extreme events in a stationary time series. In many respects, one can view the extremogram as the extreme-value analog of the autocorrelation function (ACF) of a stationary process. In classical time series modeling the ACF, and its sample counterpart, are the workhorses for measuring and estimating linear dependence in the family of linear time series processes. While the ACF has some use in measuring dependence in non-linear time series models, especially when applied to non-linear functions of the data such as absolute values and squares, it has limited value in assessing dependence between extreme events. On the other hand, the extremogram only considers observations, or groups of observations, which are large.

For a  $d$ -dimensional strictly stationary time series  $(X_t)$ , the *extremogram* is defined for two sets  $A$  and  $B$  bounded away from 0 by<sup>2</sup>

$$(1.1) \quad \rho_{A,B}(h) = \lim_{x \rightarrow \infty} P(x^{-1}X_h \in B \mid x^{-1}X_0 \in A), \quad h = 0, 1, 2, \dots,$$

provided the limit exists. Since  $A$  and  $B$  are bounded away from zero, the events  $\{x^{-1}X_0 \in A\}$  and  $\{x^{-1}X_h \in B\}$  are becoming extreme in the sense the probabilities of these events are converging to zero with  $x \rightarrow \infty$ . In the special case of a univariate time series and the choice of the sets  $A = B = (1, \infty)$ , the extremogram reduces to the (upper) tail dependence coefficient between  $X_0$  and  $X_h$  that is often used in extreme value theory and quantitative risk management; see e.g. McNeil et al. [16]. In this case, one is interested in computing the impact of a large value of the time series on a future value  $h$  time-lags ahead. With creative choices of  $A$  and  $B$ , one can investigate interesting sources of extremal dependence that may arise not only in the upper and lower tails, but also in other extreme regions of the sample space; see Sections 4 and 5 for some examples.

We would like to emphasize that the extremogram is a *conditional* measure of extremal serial dependence. Therefore it is particularly suited for financial applications where one is often interested in the persistence of a shock (an extremal event on the stock market say) at future instants of time. Another good reason for using the extremogram for financial time series is a statistical one: for large  $x$ , the quantities  $P(x^{-1}X_h \in B \mid x^{-1}X_0 \in A)$  are rare event probabilities; their non-parametric estimation cannot be based on standard empirical process techniques and requires large sample sizes. Fortunately, long financial time series are available and therefore the study of their extremal serial behavior is not only desirable but also possible. Financial time series often have the (from a statistical point of view) desirable property that they are heavy-tailed, i.e. extreme large and small values are rather pronounced and occur in clusters. The extremogram and its modifications discussed in this paper allow one to give clear quantitative descriptions of the size and persistence of such clusters.

In estimating the extremogram, the limit on  $x$  in (1.1) is replaced by a high quantile  $a_m$  of the process. Defining  $a_m$  as the  $(1 - 1/m)$ -quantile of the stationary distribution of  $|X_t|$ , the sample

---

<sup>2</sup>A set  $C$  is bounded away from zero if  $C \subset \{y : |y| > r\}$  for some  $r > 0$ .

extremogram based on the observations  $X_1, \dots, X_n$  is given by

$$(1.2) \quad \hat{\rho}_{A,B}(h) = \frac{\sum_{t=1}^{n-h} I_{\{a_m^{-1}X_{t+h} \in B, a_m^{-1}X_t \in A\}}}{\sum_{t=1}^n I_{\{a_m^{-1}X_t \in A\}}}.$$

In order to have a consistent result, we require  $m = m_n \rightarrow \infty$  with  $m/n \rightarrow 0$  as  $n \rightarrow \infty$ . In practice, we do not know  $a_m$  and therefore it has to be replaced by a corresponding empirical quantile, i.e., by one of the largest observations. Under suitable mixing conditions and other distributional assumptions that ensure the limit in (1.1) exists, it was shown in Davis and Mikosch [7] that  $\hat{\rho}_{A,B}(h)$  is asymptotically normal; i.e.,

$$(1.3) \quad \sqrt{n/m}(\hat{\rho}_{A,B}(h) - \rho_{A,B:m}(h)) \xrightarrow{d} N(0, \sigma_{A,B}^2(h)),$$

where

$$(1.4) \quad \rho_{A,B:m}(h) = P(a_m^{-1}X_h \in B \mid a_m^{-1}X_0 \in A).$$

We refer to (1.4) as the pre-asymptotic extremogram (PA-extremogram).

There are several obstacles in directly applying (1.3) for constructing confidence bands for the extremogram:

- (i) The asymptotic variance  $\sigma_{A,B}^2(h)$  is based on an infinite sum of unknown quantities and typically does not have a closed-form expression.
- (ii) Estimating  $\sigma_{A,B}^2(h)$  is similar to estimating the asymptotic variance of a sample mean from a time series and is often difficult in practice.
- (iii) The PA-extremogram cannot always be replaced by its limit.

For (i) and (ii), we turn to bootstrap procedures to approximate the distribution of  $(\hat{\rho}_{A,B}(h) - \rho_{A,B:m}(h))$ . This will allow us to construct *credible* (asymptotically correct) confidence bands for the PA-extremogram. As for (iii), a non-parametric bootstrap does not allow us to overcome the bias concern. We note, however, that the PA-extremogram is a conditional probability that is often the quantity of primary interest in applications. That is, one is typically interested in estimating conditional probabilities of *extreme* events as a measure of extremal dependence so that it is not necessary, and perhaps not even desirable to replace the PA-extremogram with the extremogram in (1.3).

The objective of this paper is to apply the bootstrap to the sample extremogram in order to overcome these limitations. By now, there are many non-parametric bootstrap procedures in the literature that are designed for use with stationary time series. Many of these involve some form of resampling from blocks of observations. That is, in constructing a bootstrap replicate of the time series, long stretches of the time series are stitched together in order to replicate the joint distributions of the process. While for a finite sample size  $n$ , it is impossible to replicate all the joint distributions, we can only sample from at most the  $m$ -variate distributions (for  $m < n$ ) by sampling blocks of  $m$  consecutive observations. In order to obtain consistency of the procedure,  $m$  is allowed to grow with  $n$  at a suitable rate. In this paper, we adopt the stationary bootstrap approach as described in Politis and Romano [18] in which the block sizes are given by independent geometric random variables. Since the blocks are of random length, the stationary bootstrap is useful as an exploratory device in which dependence beyond a fixed block length can be discovered.

In our case, there are significant differences in the extremogram setting of our bootstrap application from the traditional one. First, the summands in the numerator and denominator of (1.2)

form a triangular array of random variables and cannot be cast as a single stationary sequence. Second, most bootstrapping applications in extreme value theory, even in the iid case, require the replicate time series to be of smaller order than the original sample size  $n$ ; see e.g. Section 6.4 of Resnick [20]. On the other hand, we are able to overcome these drawbacks and show that the bootstrapped sample extremogram, based on the replicates of size  $n$  provides an asymptotically correct approximation to the left-hand side of (1.3) provided the blocks grow at a proper rate.

In addition to providing a non-parametric estimate of the nature of extremal dependence as a function of time-lag, the extremogram can also provide valuable guidance in various phases of the typical time series modeling paradigm. For example, the sample extremogram might provide insight into the choice of models for the data with the goal of delivering models that are compatible with the extremal dependence. In the standard approach, models are often selected to fit the center of the distribution and can be inadequate for describing the extremes in the data. On the other hand, if the primary interest is on modeling extremes, then the modeling exercise should focus on this aspect. The quality of fit could be judged by assessing compatibility of the sample extremogram with the fitted model extremogram. Moreover, the sample extremogram from the residuals of the model fit can be used to check compatibility with the lack of extremal dependence.

Figure 1.1 shows the sample extremograms of a GARCH(1,1) (left) and a stochastic volatility (right) process. The GARCH realization was generated from the model,

$$(1.5) \quad X_t = \sigma_t Z_t \text{ and } \sigma_t^2 = 0.1 + 0.14 X_{t-1}^2 + 0.84 \sigma_{t-1}^2,$$

where  $(Z_t)$  is an iid sequence with common distribution given by a  $t_4$  (standardized to have variance 1). The SV realization was produced from the model  $(X_t)$  satisfying

$$(1.6) \quad X_t = \sigma_t Z_t \text{ and } \log \sigma_t = 0.9 \log \sigma_{t-1} + \epsilon_t,$$

where  $(\epsilon_t)$  is a sequence of iid standard normal variables and is independent of the iid sequence  $(Z_t)$ , which has a  $t_{2.6}$  distribution. These conditions ensure that both the GARCH and SV realizations are regularly varying with index  $\alpha = 2.6$ , i.e. they have power law tails with index  $\alpha$ ; we refer to Section 2 for a precise description. For the calculation of the sample extremograms, samples of size  $n = 100,000$  were used, the sets  $A = B = (1, \infty)$  were chosen and, for  $a_m$ , the .98 empirical quantile of the simulated data was taken. It is evident from the slower decay of the sample extremogram for the GARCH(1,1) process in Figure 1.1 that this process exhibits extremal clustering while the faster decay of the sample extremogram for the SV process indicates the lack of clustering. However, without a sense for the asymptotic distribution, it is virtually impossible to make any inferences about the extremogram (pre-asymptotic or otherwise). Under the assumption of no serial dependence, one can compute permutation produced confidence bands (these are the solid lines in Figure 1.1). Clearly, the extremogram for the GARCH is significantly greater than the dashed line at height .02, which corresponds to the value of the pre-asymptotic value of the extremogram under the null hypothesis of independence. On the other hand, the extremogram for the SV process tails off after lag 18 and is not significantly different than the .02 value that one would expect for independent data. This is consistent with the theory described in Davis and Mikosch [7] in which there is extremal dependence for GARCH processes and none for SV processes. The use of permutation procedures is illustrated in more detail in Section 4.1.

The remainder of the paper is organized as follows. A brief interlude into the concept of regular variation on which the extremogram is built, is provided in Section 2. After establishing the theory

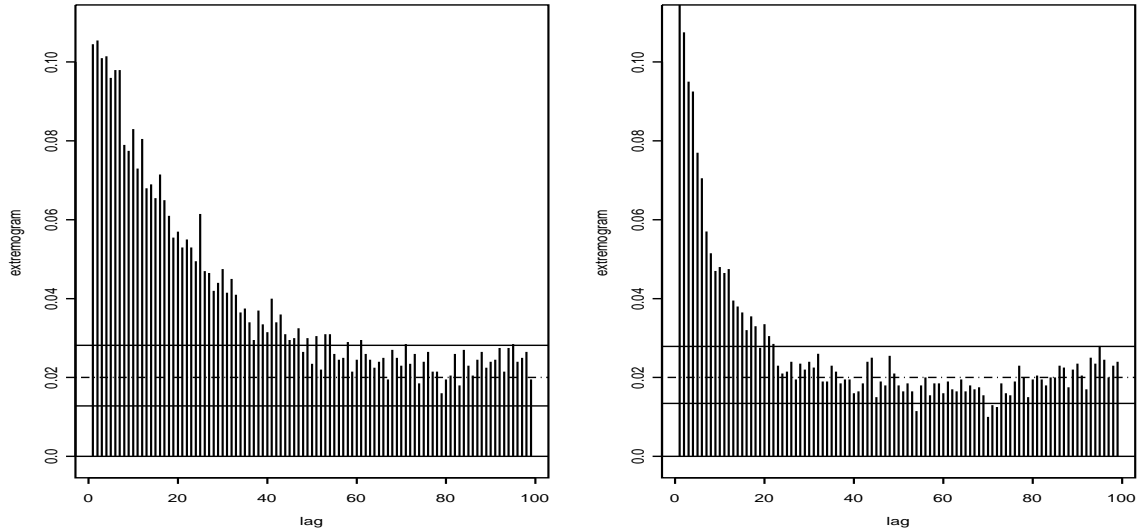


**Figure 1.1.** *The sample extremogram for the upper tail for the GARCH(1,1) (left) and SV processes (right), where the processes are specified in (1.5) and (1.6), respectively. The sample size is  $n = 100,000$  and  $a_m$  is the .98 empirical quantile. The solid horizontal lines are permutation-produced confidence bands and the dashed line at height .02 corresponds to the value of the PA-extremogram under independence.*

of the bootstrapped extremogram in Section 3, its use is demonstrated with several financial time series in Section 4. In conjunction with the bootstrapped extremogram, we present a quick and clean method for testing *significant* serial extremal dependence using a random permutation procedure. This procedure is actually similar in spirit to using the block bootstrap procedure, but with block size equal to 1. The serial dependence is completely destroyed by randomly permuting the data so that the type I error for significance of the extremogram under the null of no serial dependence can be controlled.

The cross-extremogram for multivariate time series is defined and illustrated for real data examples including the returns of the major equity indices in Section 5. Like the univariate time series, the cross-extremogram will depend on two sets, often decided upon the practitioner. We use the cross-extremogram to provide a method for assessing extremal dependence between four major international stock markets, namely, the FTSE 100, S&P 500, DAX and Nikkei 225 Indices. Without controlling for the effect of changing volatility, the cross-extremogram gives significant dependence between the series for a large number of lags. However, after devolatilizing each series using a GARCH model, the resulting extremogram shows significant dependence only at small lags. In addition, there is evidence of directionality: large values of one index follow another index.

In their presentation [13], Geman and Chang [13] consider the waiting times between rare or extreme events for financial time series. They conclude from their analysis that there is evidence of significant extremal clustering. In Section 5.4, an extremogram that calculates these return times between extreme events is defined and the sample extremogram for various time series is provided as well. Consistent with the findings of Geman and Chang the presence of extremal clustering can

be detected easily using the bootstrap. The proof of the main theorems in Section 3 is provided in the Appendix.

The reader who is mainly interested in applications of the sample extremogram to financial time series may skip the technical Sections 2 and 3 and directly go to Sections 4 and 5.

## 2. BRIEF INTERLUDE INTO REGULAR VARIATION

The extremogram (1.1) is a limit of conditional probabilities and therefore not always defined. In this section we give a sufficient condition for its existence. The condition is rather technical; the interested reader is referred to Davis and Mikosch [7] for more details. We also mention that this condition is satisfied for some of the standard financial time series models such as GARCH and SV; see [6, 7, 8, 9, 10, 15].

In this paper we focus on strictly stationary sequences whose finite-dimensional distributions have power law tails in some generalized sense. In particular, we will assume that the finite-dimensional distributions of the  $d$ -dimensional process  $(X_t)$  have *regularly varying distributions with index*  $\alpha > 0$ . This means that for any  $h \geq 1$ , the radial part  $|Y_h|$  of the lagged vector  $Y_h = \text{vec}(X_1, \dots, X_h)$  is *regularly varying with tail index*  $-\alpha$  :

$$\frac{P(|Y_h| > tx)}{P(|Y_h| > x)} \rightarrow t^{-\alpha} \quad \text{as } x \rightarrow \infty, \quad t > 0,$$

and the angular part  $Y_h/|Y_h|$  is asymptotically independent of the radial part  $|Y_h|$  for large values of  $|Y_h|$ : for every  $h \geq 1$ , there exists a random vector  $\Theta_h \in \mathbb{S}^{hd-1}$  such that

$$P(Y_h/|Y_h| \in \cdot \mid |Y_h| > x) \xrightarrow{w} P(\Theta_h \in \cdot) \quad \text{as } x \rightarrow \infty.$$

Here  $\xrightarrow{w}$  denotes weak convergence on the Borel  $\sigma$ -field of  $\mathbb{S}^{hd-1}$ , the unit sphere in  $\mathbb{R}^{hd}$  with respect to a given norm  $|\cdot|$ . The distribution  $P(\Theta_h \in \cdot)$  is called the *spectral measure* and  $\alpha$  the *index of the regularly varying vector*  $Y_h$ . We also refer to  $(X_t)$  as a *regularly varying sequence with index*  $\alpha$ .

For our purposes it will be convenient to use a sequential definition of a regularly varying sequence  $(X_t)$  which is equivalent to the definition above: there exists a sequence  $a_n \rightarrow \infty$ , an  $\alpha > 0$  and a sequence of non-null Radon measures  $(\mu_h)$  on the Borel  $\sigma$ -field of  $\overline{\mathbb{R}}_0^{hd} = \overline{\mathbb{R}}^{hd} \setminus \{\mathbf{0}\}$  such that for  $h \geq 1$ ,

$$(2.1) \quad n P(a_n^{-1} Y_h \in \cdot) \xrightarrow{v} \mu_h(\cdot),$$

where  $\xrightarrow{v}$  denotes vague convergence on the same  $\sigma$ -field; see Resnick [20], Section 6.1. The limiting measures have the property  $\mu_h(t \cdot) = t^{-\alpha} \mu_h(\cdot)$ ,  $t > 0$ . We refer to Basrak and Segers [3] who give an enlightening interpretation of the structure of a regularly varying sequence.

Now to connect the measure in (2.1) with the extremogram, for suitably chosen sets  $A$  and  $B$  in  $\mathbb{R}^d$  bounded away from the origin, set for  $h \geq 2$ ,  $\tilde{A} = A \times \mathbb{R}^{(h-1)d}$  and  $\tilde{B} = A \times \mathbb{R}^{(h-2)d} \times B$ . Provided  $\tilde{A}$  and  $\tilde{B}$  are  $\mu_h$  continuity sets, then

$$(2.2) \quad \rho_{A,B}(h-1) = \lim_{n \rightarrow \infty} P(a_n^{-1} X_h \in B \mid a_n^{-1} X_1 \in A) = \lim_{n \rightarrow \infty} \frac{n P(a_n^{-1} Y_h \in \tilde{B})}{n P(a_n^{-1} Y_h \in \tilde{A})} = \frac{\mu_h(\tilde{B})}{\mu_h(\tilde{A})}.$$

It is worth noting that standard arguments in regular variation allow one to replace  $a_n$  in the first limit appearing in (2.2) with any sequence of numbers  $x_n$  tending to  $\infty$ .

## 3. THE BOOTSTRAPPED SAMPLE EXTREMOGRAM

In this section we will construct confidence bands for the sample extremogram based on a bootstrap procedure which takes into account the serial dependence structure of the data. The resulting confidence bands closely follow the sample extremogram. Moreover, assuming regular variation of the underlying time series, we will be able to show that the bootstrap confidence bands are asymptotically correct.

**3.1. Stationary bootstrap.** This resampling scheme was introduced by Politis and Romano [18]. It is an adaptation of the block bootstrap which allows for randomly varying block sizes.

For any strictly stationary sequence  $(Y_t)$  the *stationary bootstrap procedure* consists of generating pseudo-samples  $Y_1^*, \dots, Y_n^*$  from the sample  $Y_1, \dots, Y_n$  by taking the first  $n$  elements from

$$(3.1) \quad Y_{K_1}, \dots, Y_{K_1+L_1-1}, \dots, Y_{K_N}, \dots, Y_{K_N+L_N-1},$$

where  $(K_i)$  is an iid sequence of random variables uniformly distributed on  $\{1, \dots, n\}$ ,  $(L_i)$  is an iid sequence of geometrically distributed random variables with distribution  $P(L_1 = k) = p(1-p)^{k-1}$ ,  $k = 1, 2, \dots$ , for some  $p = p_n \in (0, 1)$  such that  $p_n \rightarrow 0$  as  $n \rightarrow \infty$ , and

$$N = N_n = \inf\{i \geq 1 : L_1 + \dots + L_i \geq n\}.$$

The upper limits of the random blocks  $\{K_i, \dots, K_i+L_i-1\}$  may exceed the sample size  $n$ . Therefore, in (3.1) we replace the (unobserved)  $Y_t$ 's with  $t > n$  by the observations  $Y_{t \bmod n}$ . Finally, the three sequences  $(Y_t)$ ,  $(K_i)$  and  $(L_i)$  are also supposed independent. The dependence of the sequences  $(K_i)$  and  $(L_i)$  on  $n$  is suppressed in the notation. The generated pseudo-sample can be extended to an infinite sequence  $(Y_t^*)$  by extending (3.1) to an infinite sequence. For every fixed  $n \geq 1$ ,  $(Y_t^*)$  constitutes a strictly stationary sequence.

**3.2. Main results.** We want to apply the stationary bootstrap procedure to the strictly stationary sequence of the indicator functions  $I_t = I_{\{a_m^{-1}X_t \in C\}}$ ,  $t \in \mathbb{Z}$ , where the underlying sequence  $(X_t)$  is strictly stationary  $\mathbb{R}^d$ -valued and regularly varying with index  $\alpha$ ,  $a_m$  has the interpretation as a high quantile of the distribution of  $|X_0|$ , and  $C$  is a set bounded away from zero. The application of the stationary bootstrap in this context is rather unconventional since the sequences  $(I_t)$  constitute triangular arrays of strictly stationary sequences: through  $a_m$  these sequences also depend on  $n$ .

We write  $(I_t^*)$  for a bootstrap sequence generated from the sample  $I_1, \dots, I_n$  by the stationary bootstrap procedure described above. In what follows,  $P^*$ ,  $E^*$  and  $\text{var}^*$  denote the probability measure generated by the bootstrap procedure, the corresponding expected value and variance. This means that  $P^*(\cdot) = P(\cdot | (X_t))$  is the infinite product measure generated by the distributions of  $(K_i)$  and  $(L_i)$ .

The bootstrap sample mean  $\bar{I}_n^* = n^{-1} \sum_{i=1}^n I_i^*$  satisfies the following elementary properties:

$$E^*(\bar{I}_n^*) = E^*(I_1^*) = \bar{I}_n = n^{-1} \sum_{i=1}^n I_i,$$

$$s_n^2 = \text{var}^*(n^{1/2}\bar{I}_n^*) = C_n(0) + 2 \sum_{h=1}^{n-1} (1-h/n)(1-p)^h C_n(h),$$

where

$$C_n(h) = n^{-1} \sum_{i=1}^n (I_i - \bar{I}_n)(I_{i+h} - \bar{I}_n), \quad h = 0, \dots, n,$$

are the *circular sample autocovariances*. Here we again made use of the circular construction  $I_j = I_{j \bmod n}$ . Writing

$$\gamma_n(h) = n^{-1} \sum_{i=1}^{n-h} (I_i - \bar{I}_n)(I_{i+h} - \bar{I}_n), \quad h \geq 0,$$

for the ordinary *sample autocovariances*, we have

$$(3.2) \quad C_n(h) = \gamma_n(h) + \gamma_n(n-h), \quad h = 0, \dots, n.$$

Recall the notion of a strictly stationary regularly varying sequence from Section 2, in particular the sequence of limiting measures  $(\mu_h)$ ; see (2.1). For convenience, we write  $\mu = \mu_1$ . For any subset  $C \subset \overline{\mathbb{R}}_0^d$ , define the quantities

$$(3.3) \quad \sigma^2(C) = \mu(C) + 2 \sum_{h=1}^{\infty} \tau_h(C),$$

with  $\tau_h(C) = \mu_{h+1}(C \times \overline{\mathbb{R}}_0^{d(h-1)} \times C)$  and, suppressing the dependence on  $C$  in the notation,

$$\begin{aligned} \widehat{P}_m &= m \bar{I}_n, \quad p_0 = EI_1 = P(a_m^{-1} X_1 \in C), \\ p_{0h} &= E(I_0 I_h) = P(a_m^{-1} X_0 \in C, a_m^{-1} X_h \in C), \quad h \geq 1. \end{aligned}$$

We also need the following mixing condition:

(M) The sequence  $(X_n)$  is strongly mixing with rate function  $(\alpha_t)$ . Moreover, there exist  $m = m_n \rightarrow \infty$  and  $r_n \rightarrow \infty$  such that  $m_n/n \rightarrow 0$  and  $r_n/m_n \rightarrow 0$  and

$$(3.4) \quad \lim_{n \rightarrow \infty} m_n \sum_{h=r_n}^{\infty} \alpha_h = 0,$$

and for all  $\epsilon > 0$ ,

$$(3.5) \quad \lim_{k \rightarrow \infty} \limsup_{n \rightarrow \infty} m_n \sum_{h=k}^{\infty} P(|X_h| > \epsilon a_m, |X_0| > \epsilon a_m) = 0.$$

Our next goal is to show that the stationary bootstrap is asymptotically correct for the bootstrapped estimator of  $\widehat{P}_m$  given by

$$\widehat{P}_m^* = m \bar{I}_n^* = \frac{m}{n} \sum_{t=1}^n I_t^*.$$

The following result is the stationary bootstrap analog of Theorem 3.1 in [7]. It shows that the bootstrap estimator  $\widehat{P}_m^*$  of  $\widehat{P}_m$  is asymptotically correct.

**Theorem 3.1.** *Assume that the following conditions hold for the strictly stationary regularly varying sequence  $(X_t)$  of  $\mathbb{R}^d$ -valued random vectors:*

(1) *The mixing condition (M) and in addition*

$$(3.6) \quad \sum_{h=1}^{\infty} h \alpha_h < \infty.$$



(2) *The growth conditions*

$$(3.7) \quad p = p_n \rightarrow 0, \quad \text{and} \quad n p^2 / m \rightarrow \infty.$$

(3) *The sets  $C$  and  $C \times \overline{\mathbb{R}}_0^{d(h-1)} \times C \subset \overline{\mathbb{R}}_0^{d(h+1)}$  are continuity sets with respect to  $\mu$  and  $\mu_{h+1}$  for  $h \geq 1$ ,  $C$  is bounded away from zero and  $\sigma^2(C) > 0$ .*

(4) *The central limit theorem,  $(n/m)^{1/2} (\hat{P}_m - m p_0) \xrightarrow{d} N(0, \sigma^2(C))$  holds.*

Then the following bootstrap consistency results hold:

$$(3.8) \quad E^*(\hat{P}_m^*) \xrightarrow{P} \mu(C),$$

$$(3.9) \quad m s_n^2 = \text{var}^*((n/m)^{1/2} \hat{P}_m^*) \xrightarrow{P} \sigma^2(C),$$

with  $\sigma^2(C)$  given in (3.3). In particular

$$(3.10) \quad P^*(|\hat{P}_m^* - \mu(C)| > \delta) \xrightarrow{P} 0, \quad \delta > 0,$$

and the central limit theorem holds

$$(3.11) \quad \sup_x \left| P^*((n/m)^{1/2} (m s_n^2)^{-1/2} (\hat{P}_m^* - \hat{P}_m) \leq x) - \Phi(x) \right| \xrightarrow{P} 0,$$

where  $\Phi$  denotes the standard normal distribution function.

Politis and Romano [18] proved a corresponding result for the sample mean of the stationary bootstrap sequence  $(X_t^*)$  for a finite variance strictly stationary sequence  $(X_t)$ . They also needed the growth conditions  $p_n \rightarrow 0$  and  $n p_n \rightarrow \infty$ . Our additional condition  $(n p_n)(p_n/m) \rightarrow \infty$ , which implies  $n p_n \rightarrow \infty$  is needed since  $\hat{P}_m^*$  is an average in the triangular scheme  $I_t = I_{\{a_m^{-1} X_t \in C\}}$ ,  $t = 1, \dots, n$ . Although various steps in the proof are similar to those in Politis and Romano [18], the triangular nature of the bootstrapped sequence  $(I_t)$  requires some new ideas. We found it surprising that the full stationary bootstrap works in this context. In the context of extreme value statistics the bootstrap often needs to be modified even when the data are iid.

We now turn our attention to the sample extremograms for which both the numerator and denominator are estimators of the type  $\hat{P}_m$ . Therefore our next objective are the asymptotic properties of these ratio estimators which we study in a general context. We consider general sets  $D_1, \dots, D_h \subset \overline{\mathbb{R}}_0^d$  and  $C = D_{h+1} \subset \overline{\mathbb{R}}_0^d$ ,  $h \geq 1$ . Since we deal with several sets  $D_i$  we need to indicate that the indicator functions  $I_t$  depend on these sets:

$$I_t(D_i) = I_{\{a_m^{-1} X_t \in D_i\}}, \quad t \in \mathbb{Z},$$

and we proceed similarly for the estimators  $\hat{P}_m(D_i)$  of  $\mu(D_i)$ . Now we define the corresponding ratio estimators

$$\hat{\rho}_{C, D_i} = \frac{\hat{P}_m(D_i)}{\hat{P}_m(C)} = \frac{\sum_{t=1}^n I_{\{a_m^{-1} X_t \in D_i\}}}{\sum_{t=1}^n I_{\{a_m^{-1} X_t \in C\}}}, \quad i = 1, \dots, h.$$

Davis and Mikosch [7], Corollary 3.3, proved the joint asymptotic normality of these estimators: Note that there is a misprint for the expression for  $r_{D_i, D_j}$  in [7], which we now correct here as

$$r_{D_i, D_j} = \mu(D_i \cap D_j) + \sum_{h=1}^{\infty} [\mu_{h+1}(D_j \times \overline{\mathbb{R}}_0^{d(h-2)} \times D_i) + \mu_{h+1}(D_i \times \overline{\mathbb{R}}_0^{d(h-2)} \times D_j)].$$

The centering in the central limit theorem of Corollary 3.3 of [7] uses the PA-extremogram as opposed to the extremogram. In general the PA-extremograms cannot be replaced by their limits

$$\rho_{C,D_i} = \frac{\mu(D_i)}{\mu(C)}, \quad i = 1, \dots, h,$$

unless the following additional condition holds

$$(3.12) \quad \lim_{n \rightarrow \infty} \sqrt{nm_n} [\mu(D_i)P(a_m^{-1}X_0 \in C) - \mu(C)P(a_m^{-1}X_0 \in D_i)] = 0, \quad i = 1, \dots, h,$$

In addition to the complex form of the asymptotic variance which can hardly be evaluated, condition (3.12) points at another practical problem when applying the central limit theorem to the ratio estimators. The next result will show that these problems will be overcome by an application of the stationary bootstrap.

We construct bootstrap samples  $I_1^*(D_i), \dots, I_n^*(D_i)$ ,  $i = 1, \dots, h+1$ , from the samples  $I_1(D_i), \dots, I_n(D_i)$ ,  $i = 1, \dots, h+1$ , by a simultaneous application of the stationary bootstrap procedure, i.e., we use the same sequences  $(K_i)$  and  $(L_i)$  for the construction of the  $h+1$  bootstrap samples; see Section 3.1. From the bootstrap samples the bootstrap versions  $\hat{P}_m^*(D_i)$  of  $\hat{P}_m(D_i)$ ,  $i = 1, \dots, h+1$ , and  $\hat{\rho}_{C,D_i}^*$  of  $\hat{\rho}_{C,D_i}$ ,  $i = 1, \dots, h$ , are constructed.

The following result shows that the bootstrapped ratio estimators  $\hat{\rho}_{C,D_i}^*$  are asymptotically correct estimators of their sample counterparts  $\hat{\rho}_{C,D_i}$ ,  $i = 1, \dots, h$ .

**Theorem 3.2.** *Assume that the following conditions hold for the strictly stationary regularly varying sequence  $(X_t)$  of  $\mathbb{R}^d$ -valued random vectors:*

- (1) *The mixing conditions (M) and (3.6) hold.*
- (2) *The growth conditions (3.7) on  $p = p_n$  hold.*
- (3) *The sets  $D_1, \dots, D_{h+1}$ ,  $D_i \times \overline{\mathbb{R}}_0^{d(i-1)} \times D_i \subset \overline{\mathbb{R}}_0^{(i+1)d}$  are continuous with respect to  $\mu$  and  $\mu_{i+1}$ ,  $i = 1, \dots, h+1$ ,  $\mu(C) > 0$  and  $\sigma^2(D_i) > 0$ ,  $i = 1, \dots, h$ .*
- (4) *The central limit theorem  $(n/m)^{1/2}(\hat{\rho}_{C,D_i} - \rho_{C,D_i:m})_{i=1,\dots,h} \xrightarrow{d} N(\mathbf{0}, \Sigma)$  holds, where the asymptotic variance is defined in Corollary 3.3 of [7].*

*Then the bootstrapped ratio estimators satisfy the following bootstrap consistency result*

$$(3.13) \quad P^*(|\hat{\rho}_{C,D_i}^* - \rho_{C,D_i}| > \delta) \xrightarrow{P} 0, \quad \delta > 0,$$

*and the central limit theorem holds*

$$(3.14) \quad P^*((n/m)^{1/2}(\hat{\rho}_{C,D_i}^* - \hat{\rho}_{C,D_i})_{i=1,\dots,h} \in A) \xrightarrow{P} \Phi_{\mathbf{0},\Sigma}(A),$$

*where  $A$  is any continuity set of the normal distribution  $\Phi_{\mathbf{0},\Sigma}$  with mean zero and covariance matrix  $\Sigma$ .*

**3.3. Consistency for the bootstrapped sample extremogram.** Recall the definition of the sample extremogram  $(\hat{\rho}_{A,B}(i))$  from (1.2). This estimate can be recast as a ratio estimator by introducing the  $\mathbb{R}^{d(h+1)}$ -valued vector process

$$(3.15) \quad Y_t = \text{vec}(X_t, \dots, X_{t+h}), \quad t \in \mathbb{Z},$$

consisting of stacking  $h+1$  consecutive values of the time series  $(X_t)$ . Now the sets  $C$  and  $D_0, \dots, D_h$  specified in Theorem 3.2 are defined through the relations  $C = A \times \overline{\mathbb{R}}_0^{dh}$ ,  $D_0 = A \cap B \times \overline{\mathbb{R}}_0^{dh}$  and for  $D_i = A \times \overline{\mathbb{R}}_0^{d(i-1)} \times B \times \overline{\mathbb{R}}_0^{d(h-i)}$  for  $i \geq 1$ . With this convention, Theorem 3.2 can be applied to the

$(Y_t)$  and  $(Y_t^*)$  sequences directly. We formulate here the consistency result for the bootstrapped sample extremogram

$$\widehat{\rho}_{AB}^*(i) = \frac{\sum_{t=1}^{n-i} I_{\{a_m^{-1} X_t^* \in A, a_m^{-1} X_{t+i}^* \in B\}}}{\sum_{t=1}^n I_{\{a_m^{-1} X_t^* \in A\}}}, \quad i \geq 0.$$

We use the same notation as in Theorem 3.2.

**Corollary 3.3.** *Assume that the conditions of Theorem 3.2 are satisfied for the sequence  $(Y_t)$  and the sets  $C, D_0, \dots, D_h$  defined above. Then, conditionally on  $(X_t)$ ,*

$$(n/m)^{1/2} (\widehat{\rho}_{AB}^*(i) - \widehat{\rho}_{AB}(i))_{i=0,1,\dots,h} \xrightarrow{d} N(\mathbf{0}, \Sigma).$$

For later use, we will mention a result for the *return times extremogram*  $(\rho_A(i))$  given by the limit relations (5.2) for a fixed set  $A \subset \overline{\mathbb{R}}_0^d$  bounded away from zero and the corresponding *return times sample extremogram*  $(\widehat{\rho}_A(i))$  defined in (5.3). The bootstrapped return times sample extremogram  $(\widehat{\rho}_A^*(i))$  is defined in the straightforward way by replacing  $(X_t)$  by the stationary bootstrap sequence  $(X_t^*)$ . We again use the vector process  $(Y_t)$  defined in (3.15) and sets  $C = A \times \overline{\mathbb{R}}_0^{dh}$  and  $D_i = A \times (A^c)^{i-1} \times A \times \overline{\mathbb{R}}_0^{d(h-i)}$ ,  $i = 1, \dots, h$ , to recast  $(\widehat{\rho}_A(i))_{i=1,\dots,h}$  and  $(\widehat{\rho}_A^*(i))_{i=1,\dots,h}$ ,  $h \geq 1$ , as ratio estimators. Then Theorem 3.2 yields central limit theorems for the corresponding sample extremogram and its bootstrap version which we omit. These results show that the stationary bootstrap is asymptotically correct for the considered return times extremogram.

#### 4. EXAMPLES OF THE BOOTSTRAPPED SAMPLE EXTREMOGRAM

The first application of the bootstrapped extremogram is to the 6,443 daily log-returns of the FTSE 100 exchange from April 4, 1984 to October 2, 2009. The sample extremogram of the FTSE for lags 1 to 40 corresponding to the left tail ( $A = B = (-\infty, -1)$ ) with  $a_m$  equal to the negative of the .04 empirical quantile is displayed as the bold lines in both panels of Figure 4.1. In the left graph, the dashed lines represent .975 and .025 quantiles of the sampling distribution of  $\widehat{\rho}_{A,B}^*(h)$  based on 10,000 bootstrap replications for the daily log-returns of the FTSE. The dotted line is the mean of the bootstrapped replicates. The bootstrapped extremogram decays slowly to zero which signifies extreme serial dependence.

The right graph in Figure 4.1 shows approximate 95% confidence intervals (dashed lines) for the PA-extremogram that are found using the appropriate cutoff values from the empirical distribution of the bootstrapped replicates of  $\widehat{\rho}_{A,B}^*(h) - \widehat{\rho}_{A,B}(h)$  and the sample extremogram (dark solid line). Notice that due to the bias in the bootstrapped distribution, the sample extremogram does not fall in the center of the intervals. Using a small  $p_n$  in the bootstrapped replicates helps reduce this bias. Observe that the horizontal solid line at height .04, corresponding to a PA-extremogram under an independence assumption, is well outside these confidence bands confirming the serial extremal dependence.

The next example illustrates how the stationary bootstrap for the sample extremogram performs as a function on the choice of the mean block size. Recall from Section 3 that the condition  $p_n \rightarrow 0$  is needed in order to achieve consistency of the bootstrap estimators of the extremogram. Figure 4.2 (top left) shows the sample extremogram of the left tail for the 5-minute log-returns of Goldman Sachs (GS) from December 1, 2004 to July 26, 2006. We choose sets  $A = B = (-\infty, -1)$  and the negative of the .01 empirical quantile of the log-returns for  $a_m$ . The remaining graphs in Figure 4.2

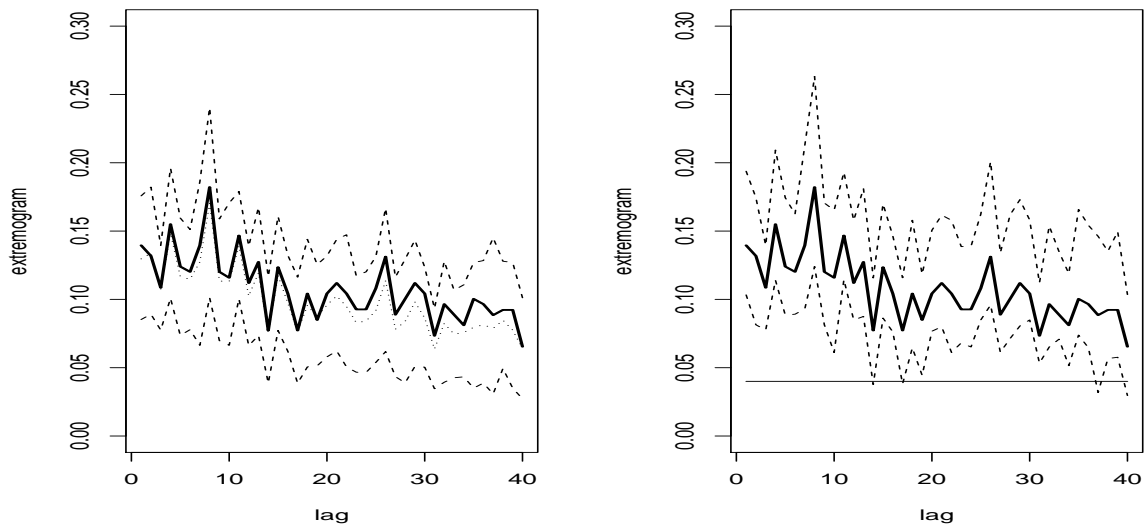


**Figure 4.1.** Left: The .975 and .025 empirical quantiles (dashed lines) of 10,000 bootstrapped replicates of the extremogram for the daily log-returns of the FTSE; the sample extremogram (solid line) and the mean of the bootstrapped replicates (dotted line). Right: 95% confidence bands (dashed lines) for the PA-extremogram based on a bootstrap approximation to the sampling distribution to the sample extremogram (solid line) and the PA-extremogram (horizontal line at .04) based on the data being independent.

show the boxplots of the sampling distribution for bootstrap replicates of the sample extremogram at just the most interesting lags of 1, 79, and 158.

The sample extremogram has a large spike at lags 79 and 158. The New York Stock Exchange (NYSE) is open daily from 9:30am to 4pm. Hence, there are 78 5-minute spells each day and so we can conclude that there is evidence of strong extremal dependence between returns a day apart. In the top right graph ( $p_n = 1/50$ ) the .975 quantiles of the distribution of the bootstrap at lags 79 and 158 do not reach the same height as in the bottom right graph ( $p_n = 1/200$ ). By resampling blocks with mean block size 50, the assumption is made that the dependence in observations  $X_t$  and  $X_{t+k}$  for  $k > 50$  has little, if any, impact on the distribution of the sample extremogram. In particular, the dependence structure is broken for lags greater than 50 and so the bootstrapped sample extremogram cannot capture the extent of the extremal dependence at lag 79 and beyond, and certainly not at lag 158.

The fixed block bootstrap is a method that resamples blocks of data of fixed length in order to keep the dependence structure intact. If such a bootstrap with fixed block size 50 was used, the opportunity to detect the extremal dependence at lags 79 and 158 would be impossible. Thus, the randomly chosen block size is a potential advantage of the stationary bootstrap: it is not unlikely to get blocks of size 90, say, if the mean block size is 50. As the mean block sizes increase from 50 to 100 to 200, the stationary bootstrap captures more and more of the dependence at lags 79 and 158.

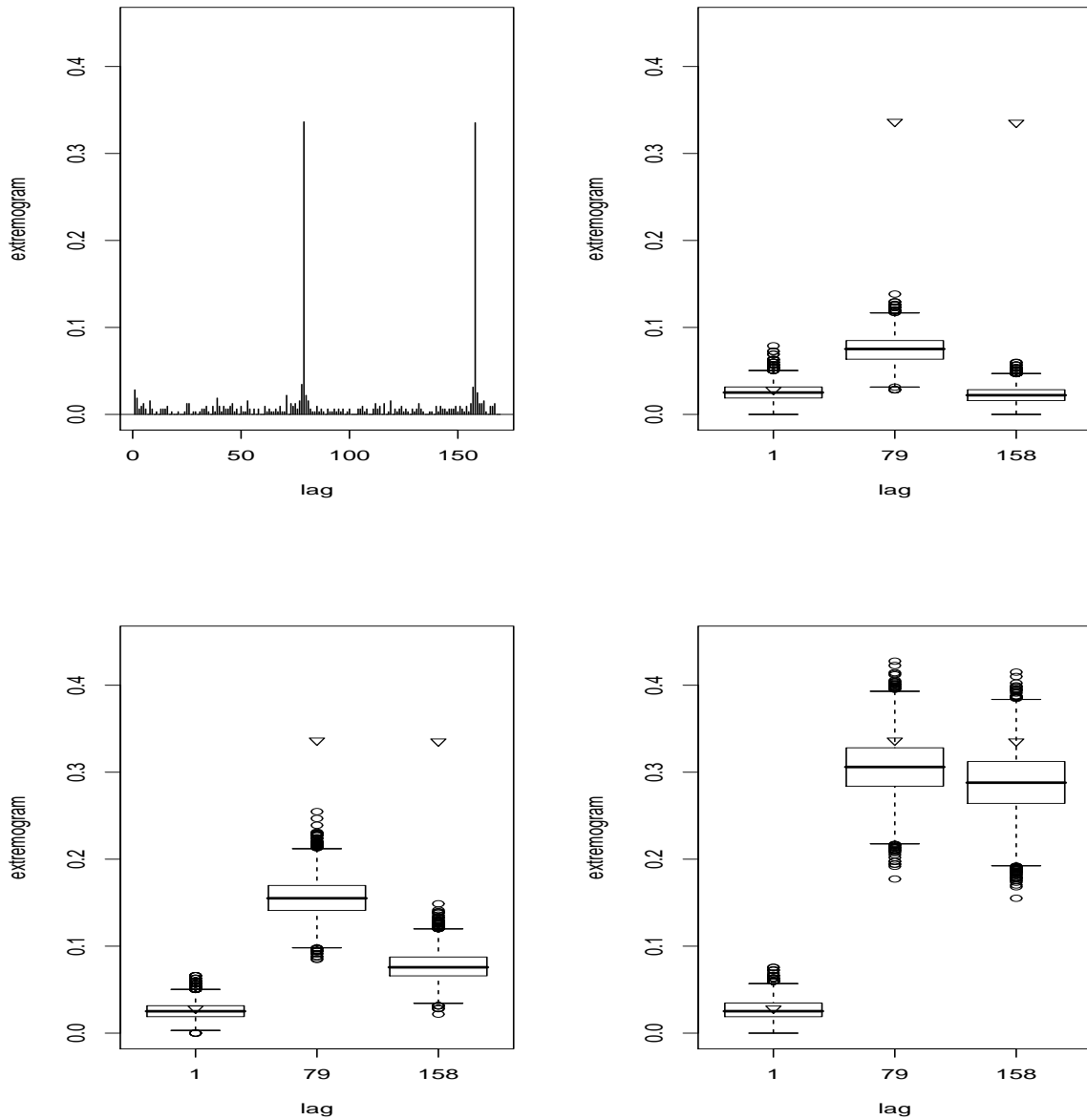


**Figure 4.2.** The sample extremogram for the 5-minute log-returns of GS (top left). Boxplots of the corresponding bootstrapped replicates of the extremograms at lags 1, 79 and 158, using a mean block size of 50 (top right), 100 (bottom left) and 200 (bottom right).

**4.1. A random permutation procedure.** We use a permutation test procedure to produce *confidence bands* for the sample extremogram under the assumption that the underlying data are in fact independent. These bounds can be viewed as the analogue of the standard  $\pm 1.96/\sqrt{n}$  bounds used for the sample autocorrelation function (ACF) of a time series. Values of the sample ACF that extend beyond these bounds lend support that the ACF at the corresponding lags are non-zero. The bounds for the sample ACF are based on well-known asymptotic theory. Unfortunately, such

bounds are not easily computable for the sample extremogram  $\hat{\rho}_{A,B}(h)$ . For a fixed lag  $h$ , if the value of the sample extremogram for the original data is not extreme relative to the values of the sample extremogram based on random permutations of the data, then the sample extremogram is impervious to the time order of the data. On the other hand, if the  $\hat{\rho}_{A,B}(h)$  is more extreme (either larger or smaller than all the extremograms computed for 99 random permutations of the data), then we conclude the presence of extremal dependence at lag  $h$  with probability  $.98=98/100$ . Aside from boundary effects, (i.e., the numerator of the sample extremogram is a sum over  $n - h$  terms and hence depends mildly on  $h$ ), the permutation distribution of the sample extremogram is virtually the same for all lags  $h$ . The bold lines in the graphs of Figure 1.1 correspond to the maximum and minimum of the sample extremogram at lag 1 based on 99 random permutations of both the GARCH (left panel) and the SV (right panel) models. The dashed line is the value of the PA-extremogram under the assumption that the data are in fact independent. In this case the value is  $.02$ . Clearly, the extremogram is measuring extremal dependence in both series.

**4.2. Equity indices.** For the next example we consider daily equity index log-returns for four countries: the United States, the United Kingdom, Germany and Japan. Here and in what follows, the indices are left in their local currencies. The top left and right graphs in Figure 4.3 show the sample extremograms for the negative tails ( $A = B = (-\infty, -1]$  with  $a_m$  estimated as the absolute value of the  $.04$  empirical quantile) applied to 6,443 daily log-returns of the FTSE 100 and S&P 500 Indices from April 4, 1984 to October 2, 2009, respectively. The bottom left and right graphs in Figure 4.3 show the analogous sample extremograms applied to 4,848 daily log-returns of the DAX Index from November 13, 1990 to October 2, 2009 and to 6,333 daily log-returns of the Nikkei 225 Index from August 23, 1984 to October 2, 2009, respectively.<sup>3</sup> The daily log-returns were calculated from the daily closing prices. Notice that the extremograms for all four indices decay rather slowly to zero, with S&P the slowest. Again the solid horizontal lines are 98% permutation produced bounds. Interestingly, the first lag in the sample extremogram for three of the indices (FTSE, DAX and Nikkei) is smaller than the second lag. Among the four indices, the Nikkei displays the least amount of extremal dependence as measured by the extremogram.

The top graphs in Figure 4.3 indicate extremal dependence in the lower tail over a period of 40 days. Typically, financial returns are modeled via a multiplication model, given by  $X_t = \sigma_t Z_t$ , where  $(Z_t)$  is an iid sequence of mean 0 variance 1 random variables and for each  $t$ , the volatility  $\sigma_t$  is independent of  $Z_t$ . It is often assumed that  $(Z_t)$  is heavy-tailed as well. Most financial time series models such as GARCH and SV, have this form. With such a model, an extreme value of the process occurs at time  $t$  if  $\sigma_t$  is large or if there is a large *shock* in the noise (i.e.,  $Z_t$ ) at time  $t$ . After estimating the volatility process  $(\sigma_t)$ , the estimated devolatilized process is defined by  $\hat{Z}_t = X_t/\hat{\sigma}_t$ . If the multiplicative model is a reasonable approximation to the return series, then the devolatilized series should be free of extremal dependence. For each of the four indices, FTSE, S&P, DAX, and Nikkei, (denoted by  $X_{t1}, X_{t2}, X_{t3}$  and  $X_{t4}$ , respectively) a GARCH(1,1) was used to devolatilize each of the four component series. Let  $\hat{Z}_{ti} = X_{ti}/\hat{\sigma}_{ti}, i = 1, \dots, 4$ , be the respective devolatilized series. Figure 4.4 shows the sample extremograms and bounds produced by the permutation procedure of the left tail for the filtered series  $\hat{Z}_{t1}$  and  $\hat{Z}_{t2}$  corresponding to

---

<sup>3</sup>As noted in the literature, the lower tails of returns tend to be heavier than the upper tails. Similar plots (not shown here) of the extremogram for the upper tails also reveal extremal dependence, but to a lesser extent than seen in the lower tails.

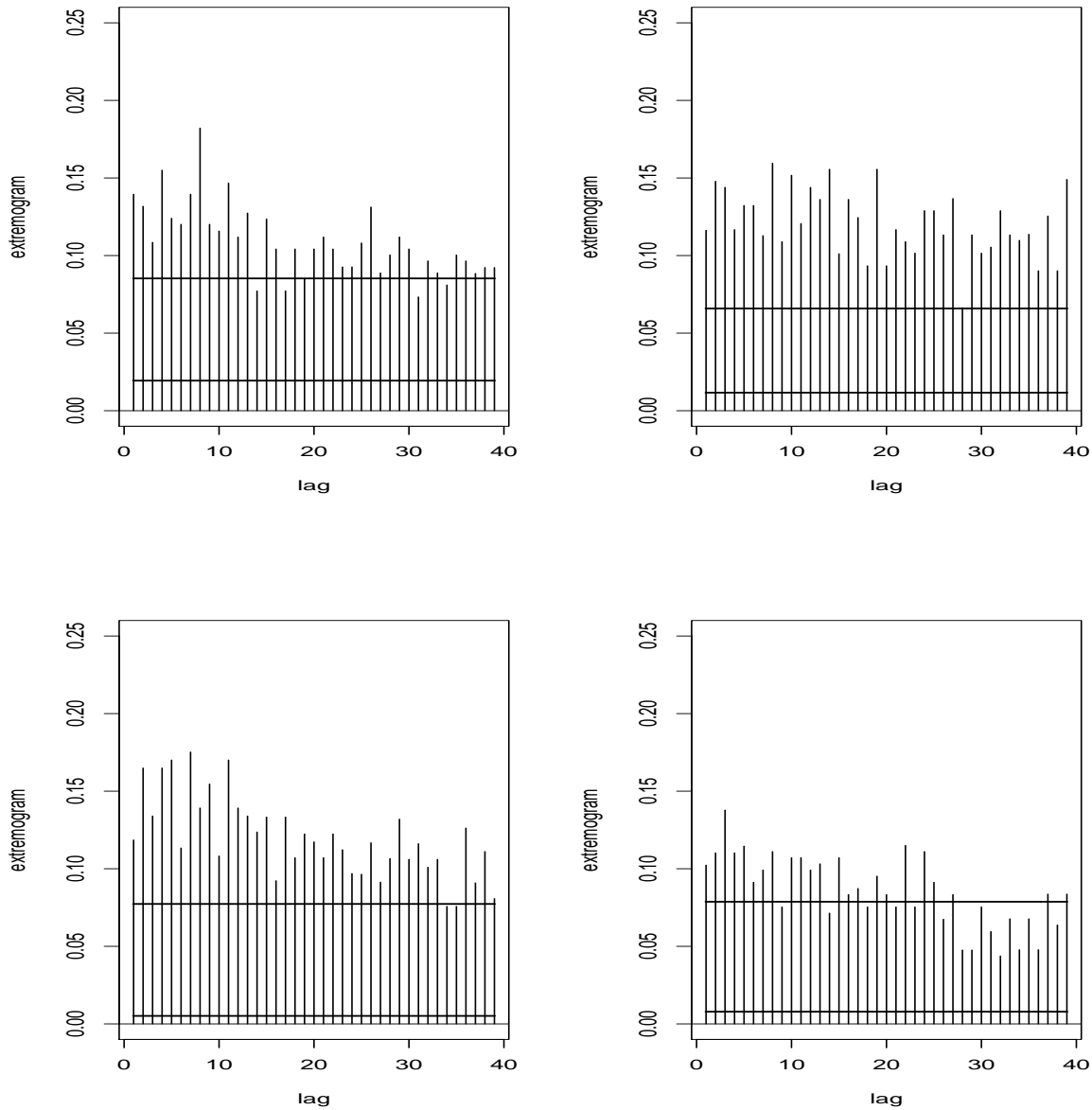


**Figure 4.3.** *The sample extremogram for the lower tails of the FTSE (top left), S&P (top right), DAX (bottom left) and Nikkei. The bold lines represent sample extremograms based on 99 random permutations of the data.*

FTSE and S&P. Here we used  $A = B = (-\infty, -1)$  and the negative of the .04 empirical quantile for  $a_m$ . These plots confirm that the extremal dependence as measured by the extremogram has been removed. Results for the filtered DAX and Nikkei are very similar. Thus the extremal dependence in the series  $(X_{ti})$  is due solely to the persistence in the volatility series.

## 5. FURTHER EXTENSIONS.

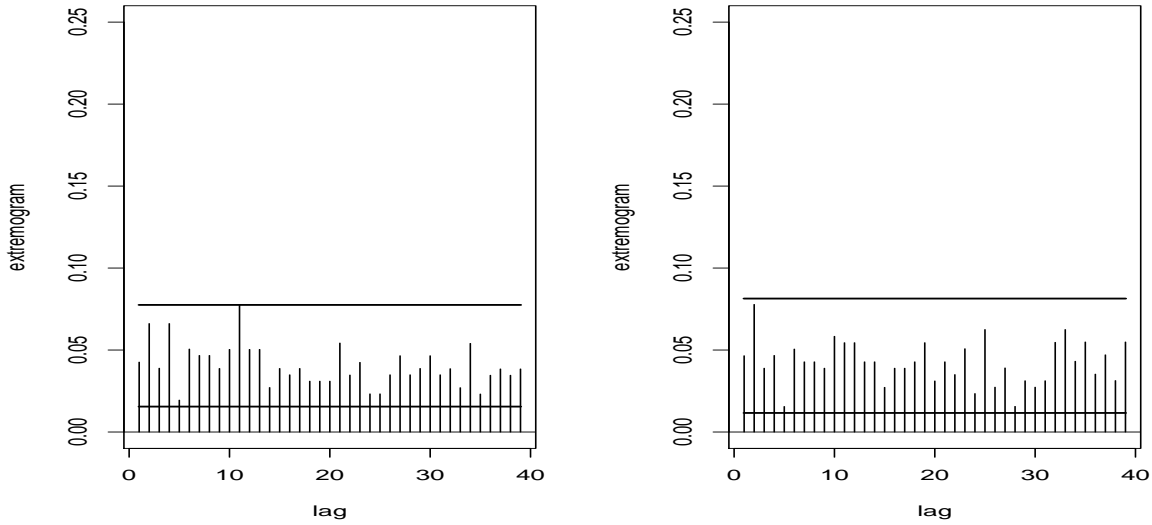


**Figure 4.4.** *The sample extremograms for the filtered FTSE (left) and the filtered S&P (right). The bold lines represent sample extremograms based on 99 random permutations of their respective filtered series.*

**5.1. Cross-extremogram for bivariate time series.** While the definition of the extremogram in (1.1) covers the case of multivariate time series, it is implicit that the index of regular variation is the same across the component series. For example, consider two regularly varying time series  $(X_t)$  and  $(Y_t)$  with tail indices  $\alpha_1$  and  $\alpha_2$  with  $\alpha_1 < \alpha_2$ . Then the bivariate time series  $((X_t, Y_t)')_{t \in \mathbb{Z}}$  would be regularly varying with index  $\alpha_1$  and

$$\lim_{x \rightarrow \infty} P(x^{-1}Y_{t+h} \in B \mid x^{-1}X_t \in A) = 0.$$

In this case, the extremogram involving the  $Y_t$  series would be zero and there would be no extremal dependence between the two component series. To avoid these rather uninteresting cases and obtain a more meaningful measure of extremal dependence, we transform the two series so that they have the same marginals. In extreme value theory, the transformation to the unit Fréchet distribution is the most standard. For the sake of argument in this discussion, assume that both  $X_t$  and  $Y_t$  are positive so that the focus of attention will be on extremal dependence in the upper tails. The case of extremal dependence in the lower tails or upper and lower tails is similar. Under the positivity constraint, if  $F_1$  and  $F_2$  denote the marginal distributions of  $X_t$  and  $Y_t$ , respectively, then the two transformed series,  $\tilde{X}_t = G_1(X_t)$  and  $\tilde{Y}_t = G_2(Y_t)$ , have unit Fréchet marginals ( $F(x) = \exp\{-1/x\}$ ,  $x > 0$ ), where  $G_i(z) = -1/\log(F_i(z))$ . Now assuming that the bivariate time series  $((\tilde{X}_t, \tilde{Y}_t)')_{t \in \mathbb{Z}}$  is regularly varying, we define the *cross-extremogram* by

$$\rho_{A,B}(h) = \lim_{x \rightarrow \infty} P(x^{-1}\tilde{Y}_h \in B \mid x^{-1}\tilde{X}_0 \in A), \quad h \geq 0,$$

where  $A$  and  $B$  are sets bounded away from 0.

At first glance, this may seem unpleasant since transformations to unit Fréchet are required. However if one restricts attention to sets  $A$  and  $B$  that are intervals bounded away from 0 or finite unions of such sets, then since  $n$  is the  $(1 - 1/n)$ -quantile of a Fréchet distribution, we have by



the monotonicity of the transformation  $G_i$ ,  $\{n^{-1}\tilde{X}_h \in A\} = \{a_{n,X}^{-1}X_h \in A\}$  and  $\{n^{-1}\tilde{Y}_h \in B\} = \{a_{n,Y}^{-1}Y_h \in B\}$ , where  $a_{n,X}$  and  $a_{n,Y}$  are the respective  $(1 - 1/n)$ -quantiles of the distributions of  $X_t$  and  $Y_t$ . So as long as the sets  $A$  and  $B$  have this form, the cross-extremogram becomes

$$(5.1) \quad \rho_{A,B}(h) = \lim_{n \rightarrow \infty} P(a_{n,Y}^{-1}Y_h \in B \mid a_{n,X}^{-1}X_0 \in A).$$

The point of this observation is that *we do not need to actually find the transformations converting the data to unit Fréchet, only the component-wise quantiles,  $a_{n,X}$  and  $a_{n,Y}$ , need to be calculated.* Clearly, this notion of extremogram extends to more than two time series.

**5.2. Sample cross-extremogram for bivariate time series.** As argued in Section 5.1, the cross-extremogram for the bivariate time series  $((X_t, Y_t))_{t \in \mathbb{Z}}$  is

$$(5.2) \quad \rho_{A,B}(h) = \lim_{m \rightarrow \infty} \rho_{A,B:m}(h) = \lim_{x \rightarrow \infty} P(a_{m,Y}^{-1}Y_h \in B \mid a_{m,X}^{-1}X_0 \in A), \quad h \geq 0,$$

where  $a_{m,Y}$  and  $a_{m,X}$  are the  $(1 - m/n)$ -quantiles of the distributions of  $|Y_t|$  and  $|X_t|$ , respectively, and  $A$  and  $B$  are finite unions of intervals that are bounded away from 0. (In cases where we only explore the upper or lower tails, we then choose  $a_{m,X}, a_{m,Y}$  to be either the  $m/n$  or the  $(1 - m/n)$ -quantiles of the respective distribution functions.) For the sake of simplicity, we use the same symbol  $\rho_{A,B}(h)$  as before, abusing notation and refer to  $\rho_{A,B:m}$  as the *pre-asymptotic cross-extremogram*.

Starting from (5.2), we define the *sample cross-extremogram* for the time series  $((X_t, Y_t))_{t \in \mathbb{Z}}$  by

$$(5.3) \quad \hat{\rho}_{A,B}(h) = \frac{\sum_{t=1}^{n-h} I_{\{a_{m,Y}^{-1}Y_{t+h} \in B, a_{m,X}^{-1}X_t \in A\}}}{\sum_{t=1}^n I_{\{a_{m,X}^{-1}X_t \in A\}}},$$

where  $a_{m,X}$  and  $a_{m,Y}$  are replaced by the respective empirical quantiles computed from  $(X_t)_{t=1,\dots,n}$  and  $(Y_t)_{t=1,\dots,n}$ , respectively.

We are interested in the extremal serial dependence in the left tail for the pairs of equity index log-returns discussed in Section 4.2. Therefore we calculate the sample cross-extremograms for these pairs with sets  $A = B = (-\infty, -1)$  and the negative .04 empirical quantiles of the returns for  $a_{m,X}$  and  $a_{m,Y}$ , respectively.

In calculating the cross-extremograms between the daily indices  $(X_{ti})$  and  $(X_{tj})$ , we only consider days  $t$  for which we have observations on both indices. Since FTSE, S&P, DAX, and Nikkei are indices from four different countries, there is not a perfect overlap on when the corresponding markets are open. The cross-extremograms between  $(X_{ti})$  and  $(X_{tj})$  exhibited a similar pattern of slow decay as seen in the univariate sample extremograms. It was thought that the strong cross-extremal dependence could be an artifact due to the persistence and synchronicity in the marginal volatilities. This phenomenon is similar in spirit to the well-known issue for the cross-correlation function of linear bivariate time series. In this case, unless one or all of the component time series have been whitened, the cross-correlation may appear to be significant (see Chapter 11 in Brockwell and Davis [4]). To explore this phenomenon, we computed the cross-extremogram for the devolatilized components. Figure 5.1 shows the sample cross-extremogram between the estimated residuals,  $\hat{Z}_{ti}$  and  $\hat{Z}_{tj}$  for  $i \neq j$  corresponding to the four indices. For example, in the first row of graphs,  $(X_t)$  is the filtered FTSE ( $\hat{Z}_{t1}$ ) and  $(Y_t)$  are the filtered S&P ( $\hat{Z}_{t2}$ ), DAX ( $\hat{Z}_{t3}$ ) and Nikkei ( $\hat{Z}_{t4}$ ), respectively. Each graph contains permutation generated confidence bands.

Interestingly, there are signs of various types of cross-extremal dependence in the filtered series. The spike at lag zero (except between the Nikkei and S&P) indicates the extremal dependence in the shocks  $\hat{Z}_{ti}$  and  $\hat{Z}_{tj}$  for  $i, j = 1, 2, 3$ . This is not surprising since we would expect dependence (extremal or otherwise) between the devolatilized series obtained from univariate GARCH(1,1) fits to each of the marginal series. In the second row, there is evidence of significant extremal dependence at lag one for each sample cross-extremogram: given the S&P has an extreme left tail shock at time  $t$  there will be a corresponding large left tail shock in the FTSE, the DAX and the Nikkei at time  $t + 1$ . Given the dominance of the US stock market, one might expect a carry-over effect of the shocks on the other exchanges on the next day. Since only marginal GARCH models were fitted to the data, it may not seem all that surprising that the filtered series exhibit serial dependence. We should note, however, that the dependence in the shocks does not appear to last beyond one time lag.

We also computed the extremogram between  $(X_{t1})$  and  $(\hat{Z}_{ti})$  for  $i = 2, 3, 4$ . These plots (not shown) were virtually identical to those displayed in Figure 5.1 which suggests that only one of the components in the cross-extremogram needs to be devolatilized.

While this analysis was carried out on the left tail, the right tail (not included) shows very similar patterns. However, the degree of dependence is different: the left tail extremal dependence probability is greater than in the right tail.

**5.3. Cross-extremogram for trivariate time series.** For a stationary trivariate regularly varying time series  $((X_t, Y_t, Z_t))_{t \in \mathbb{Z}}$ , many different variations of the cross-extremogram can be defined depending on the context. We focus on the extremograms

$$(5.4) \quad \rho_1(h) = \lim_{x \rightarrow \infty} P(\{Y_h > x\} \cup \{Z_h > x\} \mid X_0 > x), \quad h \geq 0,$$

$$(5.5) \quad \rho_2(h) = \lim_{x \rightarrow \infty} P(Z_h > x \mid \{Y_0 > x\} \cup \{X_0 > x\}), \quad h \geq 0.$$

Similar to the discussion in Section 5.1, one needs to replace the thresholds  $x$  by the quantiles of the marginal distributions if these are not identical. The sample cross-extremograms corresponding to (5.4) and (5.5), respectively, are then defined as

$$\hat{\rho}_1(h) = \frac{\sum_{t=1}^{n-h} I_{\{X_t > a_{m,1} \text{ and } (Y_{t+h} > a_{m,2} \text{ or } Z_{t+h} > a_{m,3})\}}}{\sum_{t=1}^n I_{\{X_t > a_{m,1}\}}}, \quad h \geq 0,$$

$$\hat{\rho}_2(h) = \frac{\sum_{t=1}^{n-h} I_{\{(X_t > a_{m,1} \text{ or } Y_t > a_{m,2}) \text{ and } Z_{t+h} > a_{m,3}\}}}{\sum_{t=1}^n I_{\{X_t > a_{m,1} \text{ or } Y_t > a_{m,2}\}}}, \quad h \geq 0,$$

$a_{m,i}$ ,  $i = 1, 2, 3$ , are chosen as the corresponding empirical quantiles of the  $X_t$ 's,  $Y_t$ 's and  $Z_t$ 's, respectively.

Figure 5.2 shows the sample cross-extremograms corresponding to (5.4) and (5.5). In both graphs,  $(X_t)$ ,  $(Y_t)$  and  $(Z_t)$  represent the 5-minute log-returns of Bank of America (BAC), Citibank (CBK) and Microsoft (MSFT) from December 1, 2004 to July 26, 2006, respectively. Here, the absolute values of the .96 empirical quantiles of the negative returns for the series  $(X_t)$ ,  $(Y_t)$  and  $(Z_t)$  are used for  $a_{m,1}$ ,  $a_{m,2}$  and  $a_{m,3}$ , respectively. In the left graph of Figure 5.2, one can interpret the spike at lag zero as the probability of obtaining an extreme return in either CBK or MSFT now given that there is an extreme return in BAC now. The spike at lag one has the interpretation as the probability of obtaining an extreme return in either CBK or MSFT now given that there was an extreme return in BAC 5 minutes ago. The interpretation of the spikes as lags 0 and 1 in the

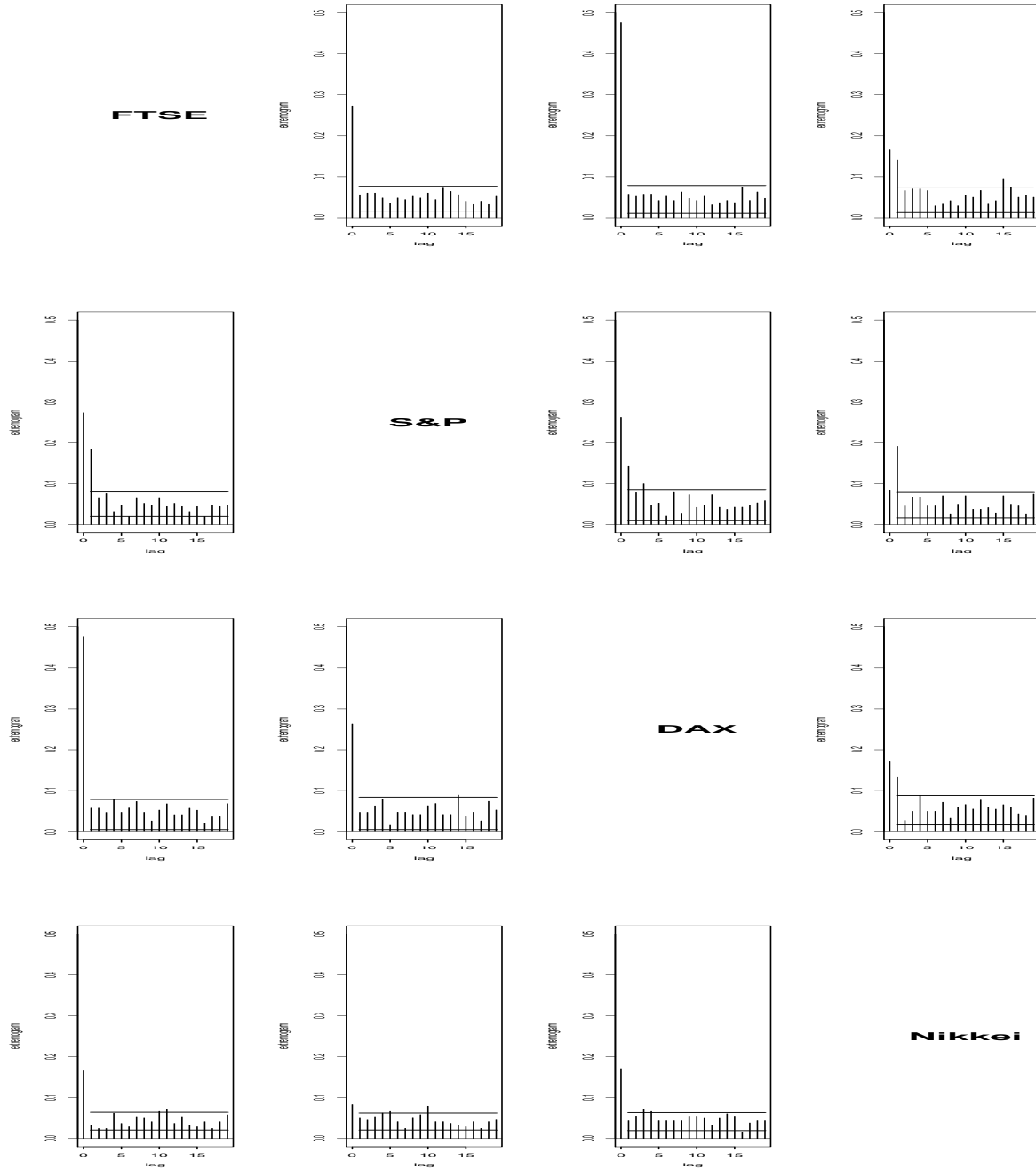


**Figure 5.1.** The sample cross-extremograms for the filtered FTSE, S&P, DAX and Nikkei series. For the first row,  $(X_t)$  is the filtered FTSE and  $(Y_t)$  are the filtered S&P, DAX and Nikkei (from left to right). For the second, third and fourth rows, the  $X_t$ 's are the filtered S&P, DAX and Nikkei series, respectively.

right graph is analogous. In both plots the decay is fast. If one wanted to utilize the information about the extremal serial dependence between the series one would have to act fast.

**5.4. The extremogram of return times between rare events.** In their presentation [13], Geman and Chang consider the waiting or return times between rare (or extreme) events for

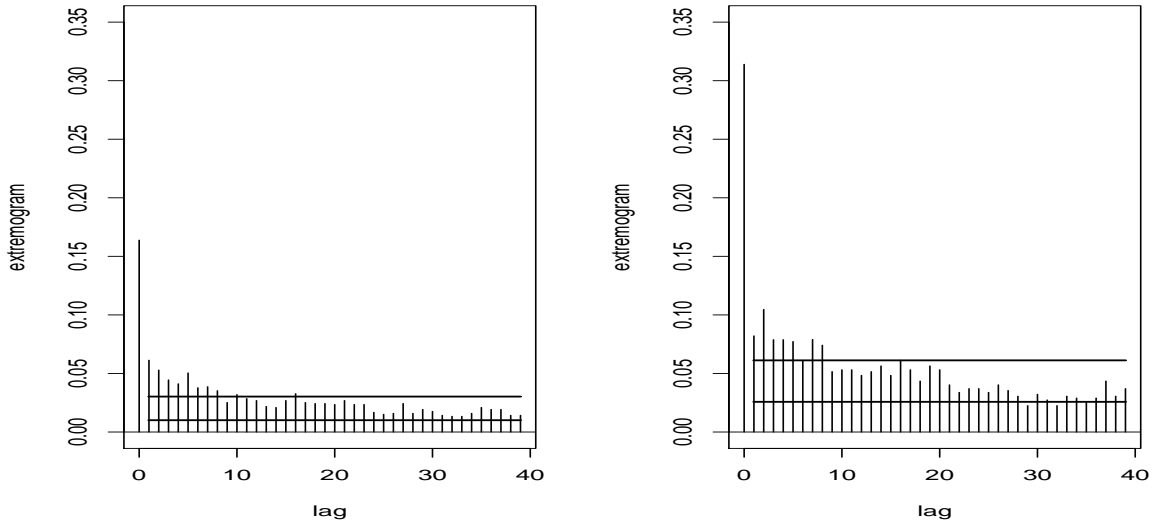


**Figure 5.2.** The sample cross-extremograms for (5.4) (left) and (5.5) (right) for the 5-minute log-returns  $X_t, Y_t, Z_t$  of BAC, CBK and MSFT, respectively.

financial time series. They define a rare event by a large excursion relative to observed returns: a return  $X_t$  is *rare* (or *extreme*) if  $X_t \leq \xi_p$  or  $X_t \geq \xi_{1-p}$ , where  $\xi_q$  is the  $q$ -quantile of the distribution of returns. Typical choices for  $p$  are 0.1 and 0.05. Denoting occurrences of rare events by the binary sequence

$$(5.1) \quad W_j = \begin{cases} 1, & \text{if } X_t \text{ is extreme,} \\ 0, & \text{otherwise,} \end{cases}$$

Geman and Chang study return times  $T_j$ ,  $j = 1, 2, \dots$ , between successive 1's of the  $W_j$  sequence. If the return times were truly iid, the successive waiting times between 1's should be iid geometric. Using the histogram of waiting times, the geometric assumption can be examined. In order to perform inference and in particular hypothesis testing on the extremal clustering of returns, Geman and Chang [13] calculate the observed entropy of the excursion waiting times and compare it to the entropies of random permutations of the excursion waiting times. If the observed entropy behaves similarly to the random permutations then one may conclude that the returns do not exhibit extremal clustering.

We now introduce an analog of the extremogram for the return times between rare events in a strictly stationary regularly varying  $\mathbb{R}^d$ -valued sequence  $(X_t)$ . Denoting the rare event by  $A \subset \overline{\mathbb{R}}_0^d$ , the corresponding return times extremogram is given by

$$(5.2) \quad \rho_A(h) = \lim_{x \rightarrow \infty} P(X_1 \notin xA, \dots, X_{h-1} \notin xA, X_h \in xA \mid X_0 \in xA), \quad h \geq 1.$$

Using the regular variation of the sequence  $(X_t)$  (see Section 2) and assuming that  $A$  and  $A \times \overline{\mathbb{R}}_0^{d(h-1)} \times A$  are continuity sets with respect to  $\mu$  and  $\mu_{h+1}$ ,  $h \geq 1$ , and  $A$  is bounded away from

zero, we can calculate the return times extremogram

$$\rho_A(h) = \frac{\mu_{h+1}(A \times \mathbb{R}^{h-1} \times A)}{\mu(A)}, \quad h \geq 0.$$

The return times sample extremogram is then defined as

$$(5.3) \quad \hat{\rho}_A(h) = \frac{\sum_{t=1}^{n-h} I_{\{a_m^{-1}X_{t+h} \in A, a_m^{-1}X_{t+h-1} \notin A, \dots, a_m^{-1}X_{t+1} \notin A, a_m^{-1}X_t \in A\}}}{\sum_{t=1}^n I_{\{a_m^{-1}X_t \in A\}}}, \quad h = 1, 2, \dots, n-1.$$

An asymptotic theory for the return times sample extremogram and its bootstrap version is given at the end of Section 3.3. This theory shows that the stationary bootstrap is asymptotically correct for this sample extremogram.

We will now illustrate some examples of the return times of extreme events. The graphs in Figure 5.3 show the histograms for the return times of extreme events for the daily log-returns of Bank of America (BAC) for different choices of the rare events  $A$ : in the left graphs  $A = \mathbb{R} \setminus [\xi_{0.05}, \xi_{0.95}]$  and in the right graphs  $A = (-\infty, \xi_{0.1})$ . The top row contains the histogram (solid vertical lines) of the log-returns, whereas the bottom row shows the corresponding histograms for the filtered time series after fitting a GARCH(1,1) model to the data; cf. Section 4.2. Since the heights of the histogram correspond exactly to the return times sample extremogram, we can apply the bootstrap procedures of Section 4. The dashed lines that overlay the graphs in Figure 5.3 represent the .975 (upper) and .025 (lower) confidence bands computed from the bootstrap approximation to the sampling distribution of the sample extremogram. The solid curve is the geometric probability mass function with success probability  $p = 0.1$ . As seen in these plots, the geometric probability mass function falls outside the confidence bands at nearly every value. This complements earlier findings of the presence of serial extremal dependence in the original daily returns.

## 6. APPENDIX: PROOFS

**6.1. Proof of Theorem 3.1.** Notice that  $E^*(\hat{P}_m^*) = \hat{P}_m$ . Now it follows from Theorem 3.1 in Davis and Mikosch [7] that

$$(6.1) \quad \hat{P}_m \xrightarrow{P} \mu(C).$$

This proves (3.8).

Next we prove (3.9), i.e., we study the asymptotic behavior of  $m s_n^2$ . Write  $\tilde{I}_t = I_t - p_0$  and

$$\begin{aligned} \tilde{C}_n(h) &= n^{-1} \sum_{i=1}^n \tilde{I}_i \tilde{I}_{i+h}, \quad h = 0, \dots, n, \\ \tilde{\gamma}_n(h) &= n^{-1} \sum_{i=1}^{n-h} \tilde{I}_i \tilde{I}_{i+h}, \quad h = 0, \dots, n-1, \end{aligned}$$

where the  $I_j$ 's in the summands are again defined circularly, i.e.,  $I_j = I_{j \bmod n}$ . Since

$$C_n(h) = n^{-1} \sum_{i=1}^n I_i I_{i+h} - (\bar{I}_n)^2 = \tilde{C}_n(h) + p_0^2 - (\bar{I}_n)^2$$

and from the central limit theorem in (4) of Theorem 3.1 and (6.1),

$$(n/m)^{1/2} m((\bar{I}_n)^2 - p_0^2) = [(n/m)^{1/2} (\hat{P}_m - m p_0)] [m^{-1} (\hat{P}_m + m p_0)] = O_P(m^{-1}),$$

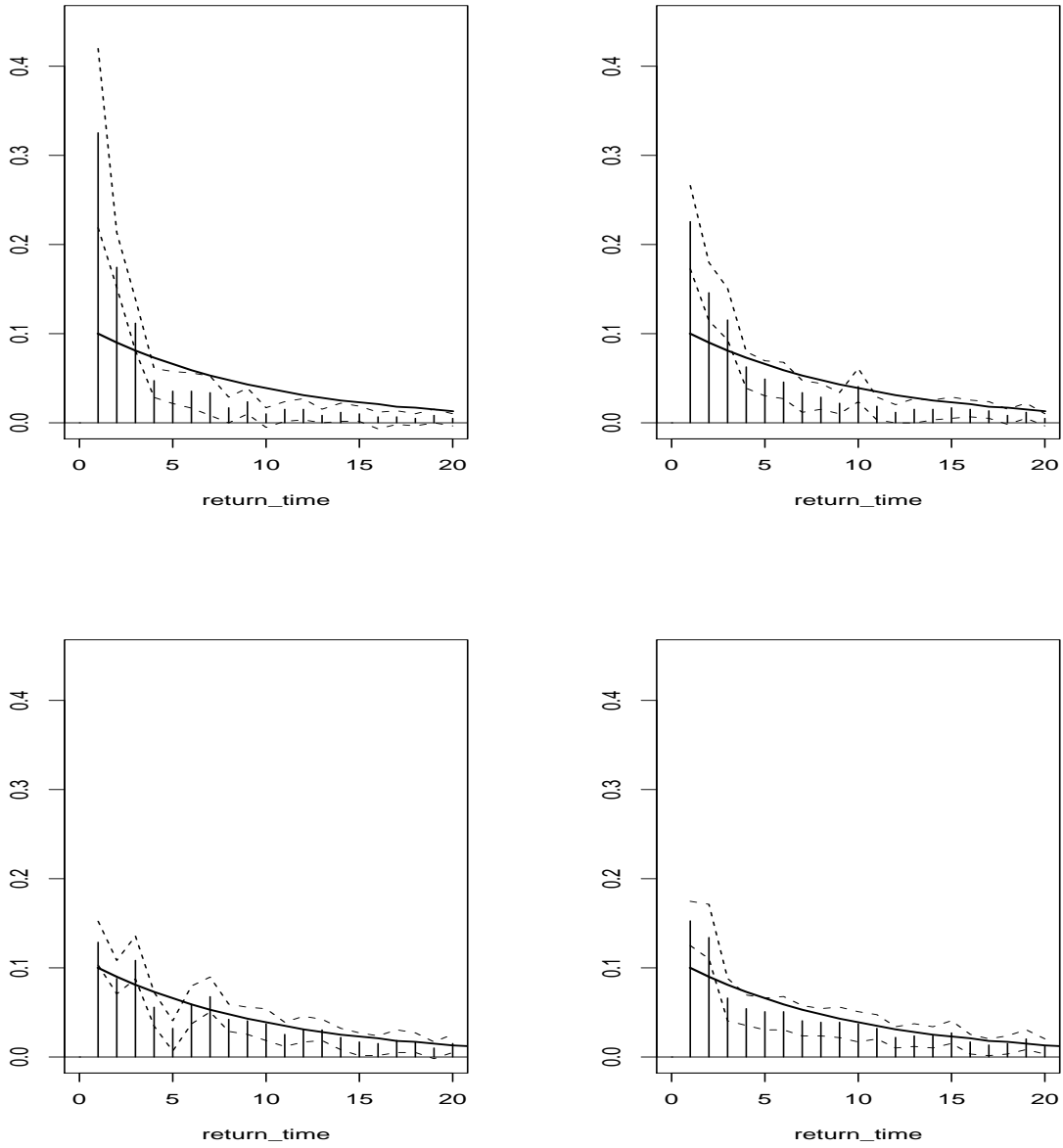


**Figure 5.3.** The histograms (solid vertical lines) for the return times of extreme events for the daily log-returns of BAC using bootstrapped confidence intervals (dashed lines), geometric probability mass function (light solid) for  $A = \mathbb{R} \setminus [\xi_{0.05}, \xi_{0.95}]$  (left) and  $A = (-\infty, \xi_{0.1})$  (right).

we have

$$\begin{aligned}
 m s_n^2 - m & \left( \tilde{C}_n(0) + 2 \sum_{h=1}^{n-1} (1 - h/n) (1 - p)^h \tilde{C}_n(h) \right) \\
 & = m((\bar{I}_n)^2 - p_0^2) \left( 1 + 2 \sum_{h=1}^{n-1} (1 - h/n) (1 - p)^h \right) \\
 (6.2) \quad & = O_P((mn)^{-1/2} p^{-1}) = o_P(1).
 \end{aligned}$$

In the last step we used assumption (3.7). It follows from (3.2) and Lemma 5.2 in Davis and Mikosch [7] that

$$(6.3) \quad m \tilde{C}_n(0) \xrightarrow{P} \mu(C) \quad \text{and} \quad m \tilde{C}_n(h) \xrightarrow{P} \tau_h(C), \quad h \geq 1.$$

We also have by assumption (3.5),

$$(6.4) \quad \lim_{k \rightarrow \infty} \limsup_{n \rightarrow \infty} E \left| m \sum_{h=k}^{r_n} (1-h/n) (1-p)^h \tilde{C}_n(h) \right| \leq \lim_{k \rightarrow \infty} \limsup_{n \rightarrow \infty} m \sum_{h=k}^{r_n} p_{0h} = 0.$$

Combining (6.2)–(6.4) and recalling the definition of  $\sigma^2(C)$  from (3.3), it suffices for (3.9) to show that for every  $\delta > 0$ ,

$$\lim_{k \rightarrow \infty} \limsup_{n \rightarrow \infty} P \left( m \left| \sum_{h=r_n}^{n-1} (1-h/n) (1-p)^h \tilde{C}_n(h) \right| > \delta \right) = 0.$$

We have

$$m \sum_{h=r_n}^{n-1} (1-h/n) (1-p)^h \tilde{C}_n(h) = \sum_{h=r_n}^{n-r_n} b_n(h) \tilde{\gamma}_n(h) + o_P(1) = T_n + o_p(1),$$

where

$$b_n(h) = m \left[ (1-h/n) (1-p)^h + (h/n) (1-p)^{n-h} \right].$$

Then

$$(6.5) \quad \begin{aligned} \text{var}(T_n) &= \sum_{h_1=r_n}^{n-r_n} \sum_{h_2=r_n}^{n-r_n} b_n(h_1) b_n(h_2) \text{cov}(\tilde{\gamma}_n(h_1), \tilde{\gamma}_n(h_2)) \\ &\leq \sum_{h_1=r_n}^{n-1} \sum_{h_2=r_n}^{n-1} b_n(h_1) b_n(h_2) \max_{r_n \leq h_1, h_2 < n-1} |\text{cov}(\tilde{\gamma}_n(h_1), \tilde{\gamma}_n(h_2))| \\ &\leq c p^{-2} m^2 \max_{r_n \leq h_1, h_2 < n-1} |\text{cov}(\tilde{\gamma}_n(h_1), \tilde{\gamma}_n(h_2))|. \end{aligned}$$

Here and in what follows,  $c$  denotes any positive constants whose value is not of interest. We have for fixed  $k$ ,

$$\begin{aligned} m^2 |\text{cov}(\tilde{\gamma}_n(h_1), \tilde{\gamma}_n(h_2))| &= (m/n)^2 \left| \sum_{t=1}^{n-h_1} \sum_{s=1}^{n-h_2} \text{cov}(I_t I_{t+h_1}, I_s I_{s+h_2}) \right| \\ &\leq c m^2/n \sum_{r=1}^n |\text{cov}(I_0 I_{h_1}, I_r I_{r+h_2})| \\ &= c(m/n) m \left( \sum_{|r-h_1| \leq k} + \sum_{k < |r-h_1| \leq r_n} + \sum_{|r-h_1| > r_n} \right) |\text{cov}(I_0 I_{h_1}, I_r I_{r+h_2})| \\ &= c(m/n) [J_1 + J_2 + J_3]. \end{aligned}$$

Using the sequential definition of the regular variation of  $(X_t)$  (see (2.1)), we have for fixed  $k$

$$\limsup_{n \rightarrow \infty} J_1 \leq \limsup_{n \rightarrow \infty} \sum_{|r-h_1| \leq k} m [p_{0,|r-h_1|} + p_0^2] \leq \sum_{h \leq k} \tau_h(C) \leq \sigma^2(C) < \infty.$$

Next we use condition (3.5):

$$\lim_{k \rightarrow \infty} \limsup_{n \rightarrow \infty} J_2 \leq \lim_{k \rightarrow \infty} \limsup_{n \rightarrow \infty} m \sum_{k < |r-h_1| \leq r_n} p_{0,|r-h_1|} + c \lim_{n \rightarrow \infty} m r_n p_0^2 = 0.$$

Finally, the mixing condition (3.4) yields

$$\limsup_{n \rightarrow \infty} J_3 \leq c \limsup_{n \rightarrow \infty} m \sum_{|r-h_1| > r_n} \alpha_{|r-h_1|} = 0.$$

Thus we proved that

$$m^2 |\text{cov}(\tilde{\gamma}_n(h_1), \tilde{\gamma}_n(h_2))| \leq c(m/n)$$

uniformly for  $h_1, h_2 \geq r_n$  and large  $n$ . We conclude from (6.5) and assumption (3.7) that

$$\text{var}(T_n) \leq c m / (n p^2) \rightarrow 0.$$

Using (3.4), it also follows that  $ET_n \rightarrow 0$ . Thus we proved that  $E(T_n^2) \rightarrow 0$ . Combining the bounds above, we conclude that (3.9) is satisfied.

Next we prove the central limit theorem (3.11). Since both sums  $\hat{P}_m^*$  and  $\hat{P}_m$  contain the same number of summands and we consider the difference  $(n/m)^{1/2}(\hat{P}_m^* - \hat{P}_m)$  we will assume in what follows that all summands  $(m/n)I_t$  in  $\hat{P}_m^*$  and  $\hat{P}_m$  are replaced by their centered versions  $(m/n)\tilde{I}_t = (m/n)(I_t - p_0)$ . We write  $\tilde{P}_m^*$  and  $\tilde{P}_m$  for the corresponding centered versions.

Write

$$(6.6) \quad \begin{aligned} S_{K_i, L_i} &= \tilde{I}_{K_i} + \cdots + \tilde{I}_{K_i + L_i - 1}, \quad i = 1, 2, \dots, \\ S_{nN} &= S_{K_1, L_1} + \cdots + S_{K_N, L_N}. \end{aligned}$$

**Lemma 6.1.** *Under the conditions of Theorem 3.1,*

$$(6.7) \quad P^*((n/m)^{1/2} |\tilde{P}_m^* - (m/n)S_{nN}| > \delta) \rightarrow 0, \quad \delta > 0.$$

*Proof.* By the argument in Politis and Romano [18] on p. 1312, using the memoryless property of the geometric distribution,  $(m/n)S_{nN} - \tilde{P}_m^*$  has the same distribution as  $(m/n)S_{K_1, L_1}$  with respect to  $P^*$ . Hence it suffices for (6.7) to show that  $(m/n)E^*(|S_{K_1, L_1}|^2) \xrightarrow{P} 0$ . An application of Markov's inequality shows that the latter condition is satisfied if

$$(6.8) \quad (m/n)E(|S_{K_1, L_1}|^2) \rightarrow 0.$$

We have by stationarity that

$$\begin{aligned} (m/n)E(|S_{K_1, L_1}|^2) &= (m/n)E(|\tilde{I}_1 + \cdots + \tilde{I}_L|^2) \\ &= (m/n) \sum_{l=1}^{\infty} \text{var}(I_1 + \cdots + I_l) (1-p)^{l-1} p. \end{aligned}$$

We have (sums over empty index sets being zero) for every fixed  $k, l \geq 1$ ,

$$\begin{aligned} m \text{var}(I_1 + \cdots + I_l) &= l \left[ m \text{var}(I_1) + 2m \sum_{h=1}^{l-1} (1-h/l) \text{cov}(I_0, I_h) \right] \\ &= l \left[ m \text{var}(I_1) + 2m \left( \sum_{1 \leq h \leq k} + \sum_{k < h \leq r_n} + \sum_{r_n < h \leq l-1} \right) (1-h/l) \text{cov}(I_0, I_h) \right]. \end{aligned}$$



The right-hand side is  $O(l)$  uniformly for  $l$  by virtue of regular variation of  $(X_t)$  and in view of the mixing condition (M). Since  $np \rightarrow \infty$  we have

$$(m/n)E(|S_{K_1, L_1}|^2) \leq c n^{-1} \sum_{l=1}^{\infty} l(1-p)^{l-1} p \leq c(np)^{-1} \rightarrow 0.$$

This proves (6.8) and finishes the proof of the lemma.  $\square$

In view of (6.7) it suffices for (3.11) to show that  $(n/m)^{1/2}[(m/n)S_{nN} - \tilde{P}_m] \xrightarrow{d} N(0, \sigma^2(C))$  conditional on  $(X_i)$ . Recall that  $E^*(S_{K_1, L_1}) = p^{-1}(\bar{I}_n - p_0)$ . Then

$$(6.9) \quad \begin{aligned} & (n/m)^{1/2} \left[ (m/n)S_{nN} - \tilde{P}_m \right] - (m/n)^{1/2} \sum_{i=1}^N (S_{K_i, L_i} - p^{-1}(\bar{I}_n - p_0)) \\ &= (np)^{-1/2} \frac{N - np}{\sqrt{np}} \left[ (n/m)^{1/2} \tilde{P}_m \right] \end{aligned}$$

The quantities  $((N - np)/\sqrt{np})$  are asymptotically normal as  $np \rightarrow \infty$  and have variances which are bounded for all  $n$ . Therefore these quantities are stochastically bounded in  $P^*$ -probability. Moreover, the quantities  $(n/m)^{1/2} \tilde{P}_m$  have bounded variances in  $P$ -probability, and therefore

$$(np)^{-1/2} [(n/m)^{1/2} \tilde{P}_m] \xrightarrow{P} 0.$$

These arguments applied to (6.9) yield for  $\delta > 0$ ,

$$P^* \left( \left| (n/m)^{1/2} [(m/n)S_{nN} - \tilde{P}_m] - (m/n)^{1/2} \sum_{i=1}^N (S_{K_i, L_i} - p^{-1}(\bar{I}_n - p_0)) \right| > \delta \right) \xrightarrow{P} 0.$$

Therefore it suffices to prove that

$$(m/n)^{1/2} \sum_{i=1}^N (S_{K_i, L_i} - p^{-1}(\bar{I}_n - p_0)) \xrightarrow{d} N(0, \sigma^2(C))$$

conditional on  $(X_i)$ . Now, an Anscombe type argument (e.g. Embrechts et al. [12], Lemma 2.5.8) combined with the asymptotic normality of  $((N - np)/\sqrt{np})$  as  $np \rightarrow \infty$  show that the random index  $N$  in the sum above can be replaced by any integer sequence  $\ell = \ell_n \rightarrow \infty$  satisfying the relation  $np/\ell \rightarrow 1$ . Given  $(X_i)$ , the triangular array

$$(m/n)^{1/2} (S_{K_i, L_i} - p^{-1}(\bar{I}_n - p_0)), \quad i = 1, \dots, \ell, \quad n = 1, 2, \dots,$$

consists of row-wise iid mean zero random variables, hence it satisfies the assumption of infinite smallness conditional on  $(X_i)$ . Therefore it suffices to apply a classical central limit theorem for triangular arrays of independent random variables conditional on  $(X_i)$ . In view of (3.9),  $\sigma^2(C)$  is the asymptotic variance of the converging partial sum sequence. Thus it suffices to prove the following Lyapunov condition conditional on  $(X_i)$ :

$$(m/n)^{3/2} \ell E^*(|S_{K_1, L_1} - p^{-1}(\bar{I}_n - p_0)|^3) \sim m^{3/2} n^{-1/2} p E^*(|S_{K_1, L_1} - p^{-1}(\bar{I}_n - p_0)|^3) \xrightarrow{P} 0.$$

An application of the  $C_r$ -inequality yields

$$\begin{aligned} & m^{3/2} n^{-1/2} p E^*(|S_{K_1, L_1} - p^{-1}(\bar{I}_n - p_0)|^3) \\ & \leq 4 m^{3/2} n^{-1/2} p \left[ E^*(|S_{K_1, L_1}|^3) + p^{-3} |\bar{I}_n - p_0|^3 \right] \\ & = 4 m^{3/2} n^{-1/2} p E^*(|S_{K_1, L_1}|^3) + 4(np)^{-2} |(n/m)^{1/2} \tilde{P}_m|^3. \end{aligned}$$

Since the last expression is  $o_P(1)$  it suffices to show that

$$(6.10) \quad m^{3/2} n^{-1/2} p E^*(|S_{K_1, L_1}|^3) \xrightarrow{P} 0.$$

An application of Markov's inequality shows that it suffices to switch to unconditional moments in the last expression. Writing  $S_l = \tilde{I}_1 + \dots + \tilde{I}_l$ , we have by stationarity of  $(X_i)$

$$E(|S_{K_1, L_1}|^3) = E(|S_{L_1}|^3) = \sum_{l=1}^{\infty} E(|S_l|^3) (1-p)^{l-1} p.$$

Next we employ a moment bound due to Rio [21], p. 54,

$$E(|S_l|^3) \leq 3\tilde{s}_l^3 + 144l \int_0^1 [\alpha^{-1}(x/2) \wedge l]^2 Q^3(x) dx,$$

where  $\alpha^{-1}$  denotes the generalized inverse of the rate function  $\alpha(t) = \alpha_{[t]}$ ,  $Q$  is the quantile function of the distribution of  $|\tilde{I}_1| = |I_1 - p_0|$  and

$$\tilde{s}_l^2 = \sum_{i=1}^l \sum_{j=1}^l |\text{cov}(I_i, I_j)| = lp_0(1-p_0) + 2 \sum_{h=1}^{l-1} (l-h) |p_{0h} - p_0^2|.$$

For every fixed  $k \geq 1$ ,

$$\tilde{s}_l^2 \leq (l/m) \left[ mp_0 + 2 \left( \sum_{h=1}^k + \sum_{h=k+1}^{r_n} + \sum_{h=r_n+1}^{l-1} \right) (1-h/l) m |p_{0h} - p_0^2| \right],$$

where sums over empty index sets are zero. Using regular variation of  $(X_i)$  and the mixing condition (M), we conclude that the right-hand side is of the order  $O(l/m)$  uniformly for  $l$ . Hence

$$\begin{aligned} m^{3/2} n^{-1/2} p \sum_{l=1}^{\infty} \tilde{s}_l^3 (1-p)^{l-1} p &\leq c n^{-1/2} p \sum_{l=1}^{\infty} l^{3/2} (1-p)^{l-1} p \\ &\leq c (np)^{-1/2} \rightarrow 0. \end{aligned}$$

Direct calculation with the quantile function of  $|\tilde{I}_t|$  shows that

$$\begin{aligned} \int_0^1 (\alpha^{-1}(x/2) \wedge l)^2 Q^3(x) dx &= p_0^3 \int_0^{1-p_0} [\alpha^{-1}(x/2) \wedge l]^2 dx + (1-p_0)^3 \int_{1-p_0}^1 [\alpha^{-1}(x/2) \wedge l]^2 dx \\ &\leq c \left[ m^{-3} \sum_{k=1}^{\infty} k \alpha_k + m^{-1} \right] = O(m^{-1}). \end{aligned}$$

In the last step we used condition (3.6). Combining the estimates above, we obtain

$$m^{3/2} n^{-1/2} p \sum_{l=1}^{\infty} E(|S_l|^3) (1-p)^{l-1} p \leq c [(np)^{-1/2} + (m/n)^{-1/2}] \rightarrow 0.$$

This proves relation (6.10) and concludes the proof of the theorem.

**6.2. Proof of Theorem 3.2.** From (3.10) we know that

$$(6.11) \quad P^*(|\widehat{P}_m^*(D_i) - \mu(D_i)| > \delta) \xrightarrow{P} 0, \quad \delta > 0, \quad i = 1, \dots, h+1,$$

therefore (3.13) follows.

Relation (6.11) implies that for each  $i = 1, \dots, h$ , in  $P^*$ -probability,

$$\begin{aligned} \widehat{\rho}_{C, D_i}^* - \widehat{\rho}_{C, D_i} &= \frac{\widehat{P}_m^*(D_i)\widehat{P}_m(C) - \widehat{P}_m^*(C)\widehat{P}_m(D_i)}{\widehat{P}_m^*(C)\widehat{P}_m(C)} \\ &= \frac{1 + o_P(1)}{\mu^2(C)} \left[ \mu(C)(\widehat{P}_m^*(D_i) - \widehat{P}_m(D_i)) - \mu(D_i)(\widehat{P}_m^*(C) - \widehat{P}_m(C)) \right]. \end{aligned}$$

Therefore it suffices for the central limit theorem (3.14) to prove a multivariate central limit theorem for the quantities  $\widehat{P}_m^*(D_i) - \widehat{P}_m(D_i)$ ,  $i = 1, \dots, h+1$ . We will show the result for  $h = 1$ ; the general case is analogous. It will be convenient to write  $D = D_1$  and  $C = D_2$ .

**Lemma 6.2.** *The following central limit theorem holds in  $P^*$ -probability*

$$\mathbf{S}_n = (n/m)^{1/2} \begin{pmatrix} \widehat{P}_m^*(D) - \widehat{P}_m(D) \\ \widehat{P}_m^*(C) - \widehat{P}_m(C) \end{pmatrix} \xrightarrow{d} N(\mathbf{0}, \Sigma),$$

where the asymptotic covariance matrix is given by

$$\begin{aligned} \Sigma &= \begin{pmatrix} \sigma^2(D) & r_{DC} \\ r_{DC} & \sigma^2(C) \end{pmatrix}, \\ r_{DC} &= \mu(C \cap D) + \sum_{i=1}^{\infty} [\mu_{i+1}(D \times \overline{\mathbb{R}}_0^{d(i-2)} \times C) + \mu_{i+1}(C \times \overline{\mathbb{R}}_0^{d(i-2)} \times D)]. \end{aligned}$$

*Proof.* We show the result by using the Cramér-Wold device, i.e.

$$\mathbf{z}'\mathbf{S}_n \xrightarrow{d} N(0, \mathbf{z}'\Sigma\mathbf{z}), \quad \mathbf{z} \in \mathbb{R}^2.$$

We indicate the main steps in the proof in which we follow the lines of the proof of Theorem 3.1. We observe that  $E^*(\mathbf{z}'\mathbf{S}_n) = 0$ . Next we show that, conditional on  $(X_t)$

$$(6.12) \quad \begin{aligned} \text{var}^*(\mathbf{z}'\mathbf{S}_n) &= (n/m) \left[ z_1^2 \text{var}^*(\widehat{P}_m^*(D)) + z_2^2 \text{var}^*(\widehat{P}_m^*(C)) + 2z_1z_2 \text{cov}^*(\widehat{P}_m^*(C), \widehat{P}_m^*(D)) \right] \\ &\xrightarrow{P} \mathbf{z}'\Sigma\mathbf{z}. \end{aligned}$$

By (3.9),  $(n/m)\text{var}^*(\widehat{P}_m^*(D)) \xrightarrow{P} \sigma^2(D)$  and  $(n/m)\text{var}^*(\widehat{P}_m^*(C)) \xrightarrow{P} \sigma^2(C)$ . Hence it suffices to show that

$$(6.13) \quad (n/m)\text{cov}^*(\widehat{P}_m^*(C), \widehat{P}_m^*(D)) \xrightarrow{P} r_{DC}.$$

We observe that

$$\text{cov}^*(\widehat{P}_m^*(C), \widehat{P}_m^*(D)) = \frac{1}{4} \left[ \text{var}^*(P_m^*(C) + \widehat{P}_m^*(D)) - \text{var}^*(P_m^*(C) - \widehat{P}_m^*(D)) \right].$$

Observe that  $P_m^*(C) \pm \widehat{P}_m^*(D)$  contain the bootstrap sequences  $I_t^*(C) \pm I_t^*(D) = (I_t(C) \pm I_t(D))^*$ ,  $t = 1, \dots, n$ . Therefore the same ideas as for Lemma 5.2 in Davis and Mikosch [7] and in the proof of Theorem 3.1 above apply to show (6.13). We omit the details.

It immediately follows from Lemma 6.1 and the argument following it that the multivariate central limit theorem can be reduced to the central limit theorem for the triangular array

$$(m/n)^{1/2} \left[ z_1 (S_{K_i, L_i}(D) - p^{-1}(\bar{T}_n(D) - p_0(D))) + z_2 (S_{K_i, L_i}(C) - p^{-1}(\bar{T}_n(C) - p_0(C))) \right],$$

$$i = 1, \dots, \ell, \quad n = 1, 2, \dots,$$

(6.14)

where  $\ell = \ell_n$  satisfies the relation  $np/\ell \rightarrow 1$ . This array consists of row-wise iid mean zero random variables, conditional on  $(X_t)$ . Relation (6.12) yields the correct asymptotic variance for the central limit theorem of the quantities (6.14). Therefore it again suffices to apply a Lyapunov condition of order 3 to the summands (6.14) conditional on  $(X_t)$ . However, an application of the  $C_r$ -inequality yields that, up to a constant multiple, this Lyapunov ratio is bounded by the sum of the Lyapunov ratios of  $S_{K_1, L_1}(C)$  and  $S_{K_1, L_1}(D)$  which, conditional on  $(X_t)$ , were shown to converge to zero in the proof of Theorem 3.1. This finishes the sketch of the proof of the theorem.  $\square$

## REFERENCES

- [1] ANDERSEN, T.G., DAVIS, R.A., KREISS, J.-P. AND MIKOSCH, T. (EDS.) (2009) *The Handbook of Financial Time Series*. Springer, Heidelberg.
- [2] BASRAK, B., DAVIS, R.A. AND MIKOSCH, T. (2002) Regular variation of GARCH processes. *Stoch. Proc. Appl.* **99**, 95–116.
- [3] BASRAK, B. AND SEGERS, J. (2009) Regularly varying multivariate time series. *Stoch. Proc. Appl.* **119**, 1055–1080.
- [4] BROCKWELL, P.J. AND DAVIS, R.A. (1991) *Time Series: Theory and Methods, 2nd edition* Springer-Verlag, New York.
- [5] DAVIS, R.A. AND MIKOSCH, T. (1998) Limit theory for the sample ACF of stationary process with heavy tails with applications to ARCH. *Ann. Statist.* **26**, 2049–2080.
- [6] DAVIS, R.A. AND MIKOSCH, T. (2001) Point process convergence of stochastic volatility processes with application to sample autocorrelations. *J. Appl. Probab.* **38A**, 93–104.
- [7] DAVIS, R.A. AND MIKOSCH, T. (2009) The extremogram: a correlogram for extreme events. *Bernoulli* **15**, 977–1009.
- [8] DAVIS, R.A. AND MIKOSCH, T. (2009) Probabilistic properties of stochastic volatility models. In: ANDERSEN, T.G., DAVIS, R.A., KREISS, J.-P. AND MIKOSCH, T. (EDS.) *The Handbook of Financial Time Series*. Springer, Heidelberg, pp. 255–268.
- [9] DAVIS, R.A. AND MIKOSCH, T. (2009) Extreme value theory for GARCH processes. In: ANDERSEN, T.G., DAVIS, R.A., KREISS, J.-P. AND MIKOSCH, T. (EDS.) *The Handbook of Financial Time Series*. Springer, Heidelberg, pp. 187–200.
- [10] DAVIS, R.A. AND MIKOSCH, T. (2009) Extremes of stochastic volatility models. In: ANDERSEN, T.G., DAVIS, R.A., KREISS, J.-P. AND MIKOSCH, T. (EDS.) *The Handbook of Financial Time Series*. Springer, Heidelberg, pp. 355–364.
- [11] DAVIS, R.A. AND RESNICK, S.I. (1989) Basic properties and prediction of max-ARMA processes. *Adv. App. Prob.* **21**, 781–803.
- [12] EMBRECHTS, P., KLÜPPPELBERG, C. AND MIKOSCH, T. (1997) *Modelling Extremal Events for Insurance and Finance*. Springer, Berlin.
- [13] GEMAN, S. AND CHANG, L.-B. (2009) Rare events in the financial markets. [http://www.dam.brown.edu/people/geman/Homepage/Some recent stuff/Rare Events.pdf](http://www.dam.brown.edu/people/geman/Homepage/Some%20recent%20stuff/Rare%20Events.pdf).
- [14] LEADBETTER, M.R., LINDGREN, G. AND ROOTZÉN, H. (1983) *Extremes and Related Properties of Random Sequences and Processes*. Springer, Berlin.
- [15] LINDNER, A. (2009) Stationarity, mixing, distributional properties and moments of GARCH( $p, q$ )-processes. In: ANDERSEN, T.G., DAVIS, R.A., KREISS, J.-P. AND MIKOSCH, T. (EDS.) (2009) *The Handbook of Financial Time Series*. Springer, Heidelberg.

- [16] MCNEIL, A., FREY, R. AND EMBRECHTS, P. (2005) *Quantitative Risk Management: Concepts, Techniques, and Tools*. Princeton Series in Finance. Princeton University Press, Princeton NJ.
- [17] MIKOSCH, T. AND STĂRICĂ, C. (2000) Limit theory for the sample autocorrelations and extremes of a GARCH(1,1) process. *Ann. Statist.* **28**, 1427–1451.
- [18] POLITIS, D.N. AND ROMANO, J.P. (1994) The stationary bootstrap. *J. Amer. Statist. Assoc.* **89**, 1303–1313.
- [19] RESNICK, S.I. (1987) *Extreme Values, Regular Variation, and Point Processes*. Springer, New York.
- [20] RESNICK, S.I. (2007) *Heavy-Tail Phenomena: Probabilistic and Statistical Modeling*. Springer, New York.
- [21] RIO, E. (1994) About the Lindeberg method for strongly mixing sequences. *ESAIM: Probability and Statistics* **1**, 35–61.

DEPARTMENT OF STATISTICS, COLUMBIA UNIVERSITY, 1255 AMSTERDAM AVE. NEW YORK, NY 10027, U.S.A.  
*E-mail address:* rdavis@stat.columbia.edu , www.stat.columbia.edu/~rdavis

DEPARTMENT OF MATHEMATICS, UNIVERSITY OF COPENHAGEN, UNIVERSITETSPARKEN 5, DK-2100 COPENHAGEN, DENMARK  
*E-mail address:* mikosch@math.ku.dk , www.math.ku.dk/~mikosch

DEPARTMENT OF STATISTICS, COLUMBIA UNIVERSITY, 1255 AMSTERDAM AVE. NEW YORK, NY 10027, U.S.A.  
*E-mail address:* ivor@stat.columbia.edu